REPORT DOCUMENTATION PAGE

Form Approved OMB No. 0704-0188

1. REPORT DATE *(DD-MM-YYYY)*	2. REPORT TYPE	3. DATES COVERED *(From – To)*
28-05-2003	Final Report	1 May 2002 - 01-May-03

4. TITLE AND SUBTITLE

Polymers used as Fuel for Laser Plasma Thrusters in Small Satellites

5a. CONTRACT NUMBER
F61775-02-WE038

5b. GRANT NUMBER

5c. PROGRAM ELEMENT NUMBER

6. AUTHOR(S)

Dr. Thomas Lippert

5d. PROJECT NUMBER

5d. TASK NUMBER

5e. WORK UNIT NUMBER

7. PERFORMING ORGANIZATION NAME(S) AND ADDRESS(ES)
Paul Scherrer Institut
Villigen PSI CH-5232
Switzerland

8. PERFORMING ORGANIZATION REPORT NUMBER

N/A

9. SPONSORING/MONITORING AGENCY NAME(S) AND ADDRESS(ES)

EOARD
PSC 802 BOX 14
FPO 09499-0014

10. SPONSOR/MONITOR'S ACRONYM(S)

11. SPONSOR/MONITOR'S REPORT NUMBER(S)
SPC 02-4038

12. DISTRIBUTION/AVAILABILITY STATEMENT

Approved for public release; distribution is unlimited.

13. SUPPLEMENTARY NOTES

14. ABSTRACT

This report results from a contract tasking Paul Scherrer Institut as follows: The contractor will investigate those properties of promising polymers which influence the performance of Laser Plasma Thrusters LPTs). Preliminary data show that the properties of the ablated polymer have a strong efect on the achievable specific impulse. Among the issues to be investigated are choice of substrate and adhesion of the polymer to the substrate, influence of dopants to increase optical absorption, and thickness of the polymer layer.

15. SUBJECT TERMS
EOARD, Polymer Chemistry, Laser plasmas, laser propulsion

16. SECURITY CLASSIFICATION OF:			17. LIMITATION OF ABSTRACT	18, NUMBER OF PAGES	19a. NAME OF RESPONSIBLE PERSON
a. REPORT	b. ABSTRACT	c. THIS PAGE			Alexander J. Glass, Ph.D.
UNCLAS	UNCLAS	UNCLAS	UL	49	19b. TELEPHONE NUMBER *(Include area code)* +44 (0)20 7514 4953

FINAL REPORT

Project SPC 02-4038 with contract order number F61775-02-WE-038

for the time period May 1 2002 to April 30, 2003

Thomas Lippert

Paul Scherrer Institut 5232 Villigen PSI, Switzerland

Polymers used as Fuel for Laser Plasma Thrusters in Small Satellites

Declarations, Acknowledgements and Clauses

1. "252.235-7010 ACKNOWLEDGMENT OF SUPPORT AND DISCLAIMER."

Acknowledgement of Support: This material is based upon work supported by the European Office of Aerospace Research and Development, Air Force Office of Scientific Research, Air Force Laboratory, under contract F61775-01-WE057.

Disclaimer: Any opinions, findings and conclusions or recommendations expressed in this material are those of the authors and do not necessarily reflect the views of the European Office of Aerospace Research and Development, Air Force Office of Scientific Research, Air Force Laboratory.

2. "THE FINAL REPORT DELIVERED UNDER THIS CONTRACT SHALL INCLUDE OR ADDRESS THE FOLLOWING TWO ITEMS."

(1) In accordance with Defense Federal Acquisition Regulation 252.227-7036, Declaration of Technical Data Conformity (Jan 1997), All technical data delivered under this contract shall be accompanied by the following written declaration:

"The Contractor, Induced Gamma Emission Foundation, hereby declares that, to the best of its knowledge and belief, the technical data delivered herewith under Contract No. F61775-00-WE056 is complete, accurate, and complies with all requirements of the contract."

DATE: _April 30, 2003_____

Name and Title of Authorized Official:
PD Dr. Thomas Lippert

_____

(2) In accordance with the requirements in Federal Acquisition Regulation 52.227-13, Patent Rights-Acquisition by the U.S. Government (Jun 1989),

CONTRACTOR WILL INCLUDE IN THE FINAL REPORT ONE OF THE FOLLOWING STATEMENTS:

(B) "I certify that there were no subject inventions to declare as defined in FAR 52.227-13, during the performance of this contract."

DATE: April 30, 2003_____

Name and Title of Authorized Official:

PD Dr. Thomas Lippert

_____

RESULTS

The studies in this project were performed in close cooperation with Claude Phipps (Photonic Associates, Santa Fe, NM), who works on the more applied and testing related aspects of the application of laser plasma microthrusters (LPT). The work of Claude Phipps is supported by the U.S. Air Force under contracts F04611-02-M-0025, F49620-00-C-0005, and F49620-980C-0038. The material optimization, selection, and sample preparation was performed in close cooperation with Claude Phipps to optimize the performance of polymer films in LPT's and to understand the differences determined for different materials, by studying the polymers with various techniques, e.g. time-resolved measurements. The overall goal is to obtain design criteria for improving the performance of the polymer films, including the preparation for tapes, in LPT's.

Results I: Material Research

In the first part of this project various material aspects have been studied, i.e. the selection and preparation of the polymers films on the transparent polymeric substrates. Most polymers do not have an absorption in the near IR, except some special polymers, e.g. polyaniline (see scheme 1).

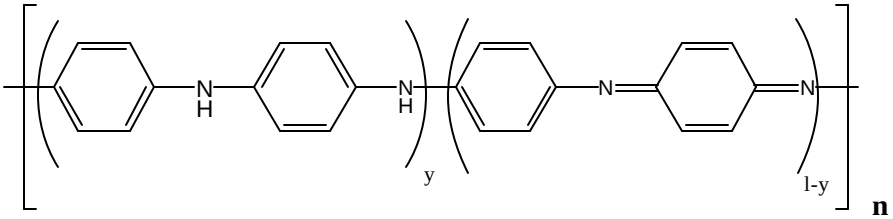

Emeraldine base

Scheme 1: Structural unit of polyaniline in the form of the emeraldine base.

Unfortunately it was impossible to develop a procedure to create films with a thickness of 70 to 150 micron on one of the selected substrate materials, i.e. polyimide, polyethylenterephthalate, or acetate. Therefore we decided to dope the polymers with materials, which absorb in the near IR (at 935 nm) where the laser diodes emit.

Two possibilities exist for creating an absorption in the near IR, i.e. by broadband absorption over the whole visible to near IR region of the spectrum by using carbon, or by using IR absorbing dyes. The latter should in principle be the better choice, because the molecular dye should create a very homogeneous transfer of the laser energy to the surrounding polymer matrix. IR dyes are not very common and only one supplier could be identified (Epolin, INC, 358-364 Adams Street, Newark, NJ 07105, USA). We selected two dyes (Epolight III 178 = IR-165 and Epolight III 192), one of them has been applied by other groups[1] as molecular heater (IR-165). A technique was developed to create films with the IR dyes, but the homogeneity was not really satisfying. Additionally another problem was encountered, i.e. the dyes decomposed upon storage in light. Epolin offers now new, sun light stable dyes. We selected and purchased two of them (Epolight 2057 and 3138) and will try to develop a procedure for the preparation of films in the near future (described below).

Simultaneously we developed procedures for films doped with carbon. For this experiments 4 different types of carbon were selected (basic, acidic, and conducting carbon soot, plus carbon nanopearls with a nominal particle size of 5-10 nm). A standard polymer was used (Alocotex 97 = polyvinylalcohol-polyethylenglycol copolymer) as matrix, because the energetic polymers are more difficult to prepare. Samples were prepared and sent to C. Phipps, who performed experiments to measure the momentum coupling coefficient and specific impulse. The best performance was obtained for the carbon nanopearls, which will be used now for all future experiments.

Carbon is probably also the material of choice for the “best” energetic polymers, as the preparation of these films involves several steps that include chemical reactions (crosslinking), and the stability of the IR dye during these reactions is doubtful.

We have also prepared large coated films for Claude Phipps, which are used for the preparation of fuel tapes. The group of Claude Phipps had recently identified

---

[1] X. Wen, D. E. Haare, D. D. Dlott, Appl. Phys. Lett. **64**, 184 (1994).

that acetate is the best substrate material, due to the high transparency (resistivity) for IR irradiation. Therefore, we tried to prepare films (our “best” energetic polymer with carbon nanopearls) on acetate. The solvent used for the polymer film preparation is unfortunately also a solvent for the acetate substrate. This results in wavy films, where even the substrate material becomes brittle and therefore impossible to use in the “tape-geometry”. As an alternative the second best substrate material was selected (polyimide) where smooth, large films could be prepared. The films were quite thick (300 to 500 micron), but thrust of up to 455 μN, C_m of 330 μN/watt and I_{sp} of only 100 s were obtained. In the previous “static” (non-tape) experiments I_{sp} of up to 550 s could be obtained. We believe that the difference might be due to the much thicker films in the “tape” measurements, which causes problems for the experimental setup (high numerical aperture lens of 0.68, results in a pronounced beam diameter increase over the film thickness). Thinner samples for the “tape” tests revealed a substantial improvement in C_m when 370 micron thick coatings were compared to 140 micron coatings, i.e. from 42 to 64 dyn W^{-1}.

We also modified our film preparation procedure to minimize the outgassing of the films. Improvements could be obtained, e.g. by drying the films in a vacuum oven.

Results II: Shadowgraphy and Emission-Spectroscopy

The influence of the polymer properties on the obtained performance was studied systematically by selecting three different polymers and the above described preparation procedure. These films were sent to Dr. Claude Phipps, who measured the specific impulse and momentum coupling coefficients. We selected 3 polymers for further studies:

Polyvinylchloride (PVC): Material selected by Claude Phipps. PVC had the best performance among the commercial polymers (better or at least equal to TP).

Triazene-Polymer (TP): One of our materials developed for laser structuring in the UV (better performance in the thrust experiments than most commercial polymers, except PVC).

Energetic Polymer (EP/GAP). Polymer based on GAP, the “best” performer in the thruster tests (by Claude Phipps). The chemical structures are shown in Scheme 2.

The polymers were studied with two different techniques, i.e. time-resolved shadowgraphy and time-resolved emission spectroscopy at various irradiation

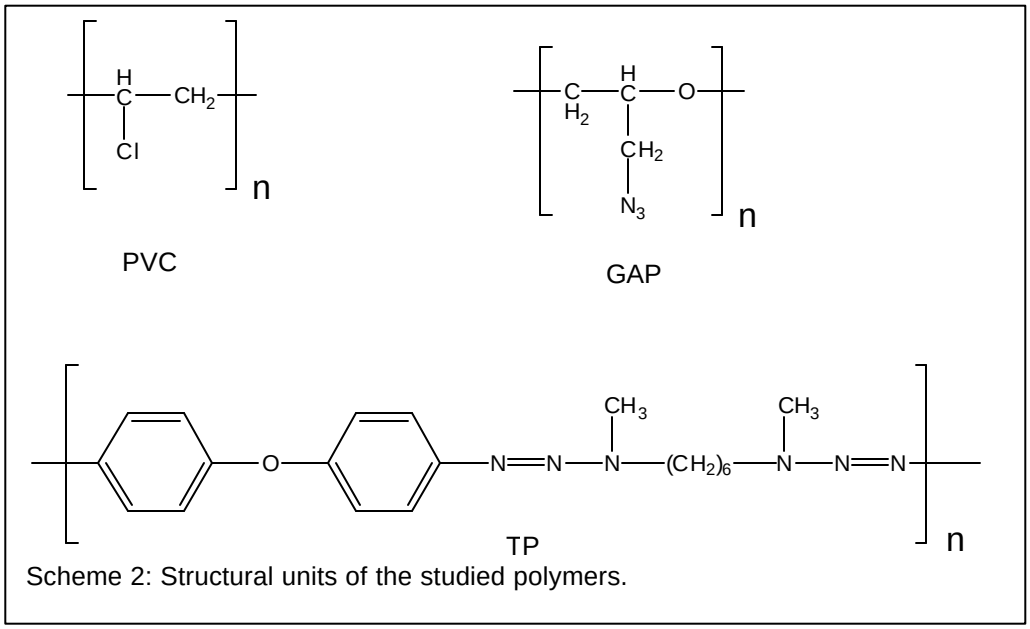

Scheme 2: Structural units of the studied polymers.

wavelengths. Different irradiation wavelengths were applied to study whether clear influences of the energy transfer mechanism (from the dopant, e.g. carbon, to the polymer matrix) can be detected. Irradiation at wavelengths which are directly absorbed by the polymer (i.e. 193 nm) should give clear indications about properties of the “pure” polymer matrix.

The irradiations were performed and studied over a broad fluences range, i.e. from the begin of ablation to fluences were a plasma can be observed.

From time-resolved shadowgraphy measurements information about the shock wave propagation in air and the state of the products are obtained. These experiments were performed at 193 nm (directly absorbed by all polymers), 308 nm (only directly absorbed by TP), 532 nm (all polymers absorb only after doping with carbon) and 1064 nm (all polymers absorb only after doping with carbon). We implemented (developed) also an experimental setup to use diode lasers (supplied by Claude Phipps), but the diodes were unfortunately defect. Therefore

no data on irradiation with IR diodes and various pulse lengths could be obtained.

Two different setups for shadowgraphy were tested:

- In Mach-Zehnder geometry (data for 193 nm and 308 nm irradiation). This setup has the principle advantage that it will allow (with our analysis routine) to determine the plume transmission and, in the case of a plasma, electron densities. The “raw” data are more difficult to interpret, therefore we decided to apply for the initial experiments an easier setup, i.e.
- Classical shadowgraphy, where a dye cell is used as back illumination (shown in Figure 1). The dye is either pumped at 532 nm (for UV irradiation of the polymers, 30 ns FWHM) or at 308 nm (for 532 and 1064 nm irradiation of the polymers, 6 ns FWHM). The dye acts as flashlight, with flashes in the range of 7 ns, while a C-MOS camera with zoom objective and open shutter times in the microsecond range is used. The two lasers (irradiation of the polymer and pumping of the dye cell or to create the interference fringes parallel to the polymer surface in the case of the Mach-Zehnder setup) are synchronized by a delay generator which allows to record time resolved shadowgraphy.

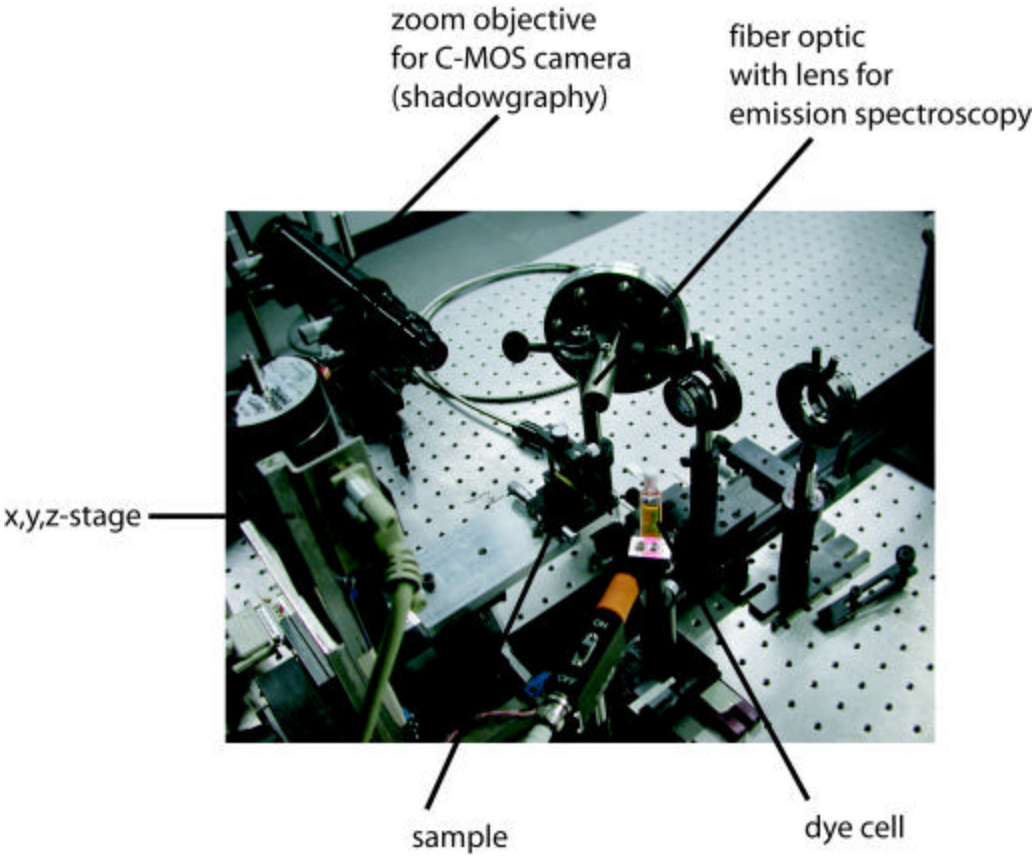

Figure 1: Photo of the experimental setup.

A comparison of shadowgraphy images at one time delay for the irradiation at various wavelengths is shown in Figure 2. The surface of the polymer was irradiated directly, also called front side irradiation (laser pulse from the left side). The top 4 pictures are recorded with the Mach-Zehnder setup, while the two images at the bottom are created with the classical shadowgraphy setup. The quality of the last images is clearly better than for the Mach-Zehnder images. The two images at the top show the irradiation of the triazene-polymer at 193 and 308 nm. The polymer absorbs these two irradiation wavelengths directly, and it was only possible to detect a pronounced shock wave in air, but NO solid ablation products. The same behavior is observed for GAP (energetic polymer) for 193 nm irradiation (directly absorbed, shown with added carbon, but the same behavior is also observed for “pure” EP samples). For 308 nm irradiation a different behavior is observed (middle picture in the right row). A darkened area is visible just above the polymer surface, which probably corresponds to larger

ablation fragments or a very dense gaseous ablation cloud. Irradiation at 532 and 1064 nm results in a later ejection of solid fragments (with a larger amount of larger particles in the case of 1064 nm).

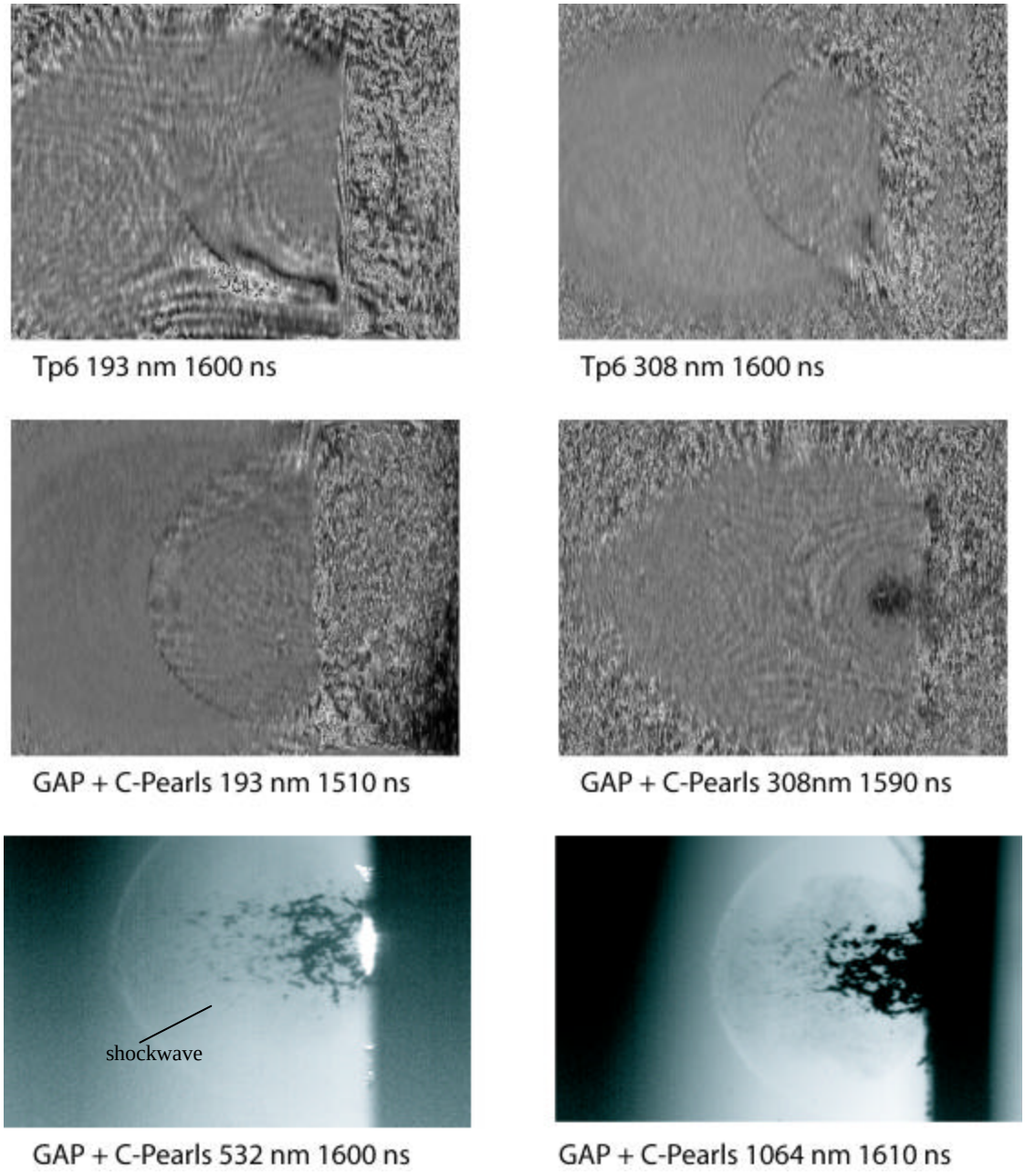

Figure 2: Comparison of the shadowgraphy images for different irradiation wavelength.

The evolution of the materials ejection is shown in Figure 3 for EP and irradiation at 1064 nm. The ejected material and the shock wave in air are clearly visible at

around 210 ns after the pump pulse. At later stages the ejected material seems to condense and may consist of molten material.

In Figure 4 the same experiment is shown, but with a different irradiation geometry. In this case the irradiation laser (1064 nm) comes again from the left side, but the EP film is irradiated through the transparent substrate. This geometry corresponds to geometry used by Claude Phipps in his micro thruster setup. A different behavior is observed in these experiments. A pronounced swelling of the polymer film until 2500 ns is observed, followed by a volcano-like eruption (the different appearance between the last two pictures is probably due to different film thicknesses between the two experiments-as all pictures are single-shot experiments with new sample position for each measurement). Also in this case a shock wave is clearly visible.

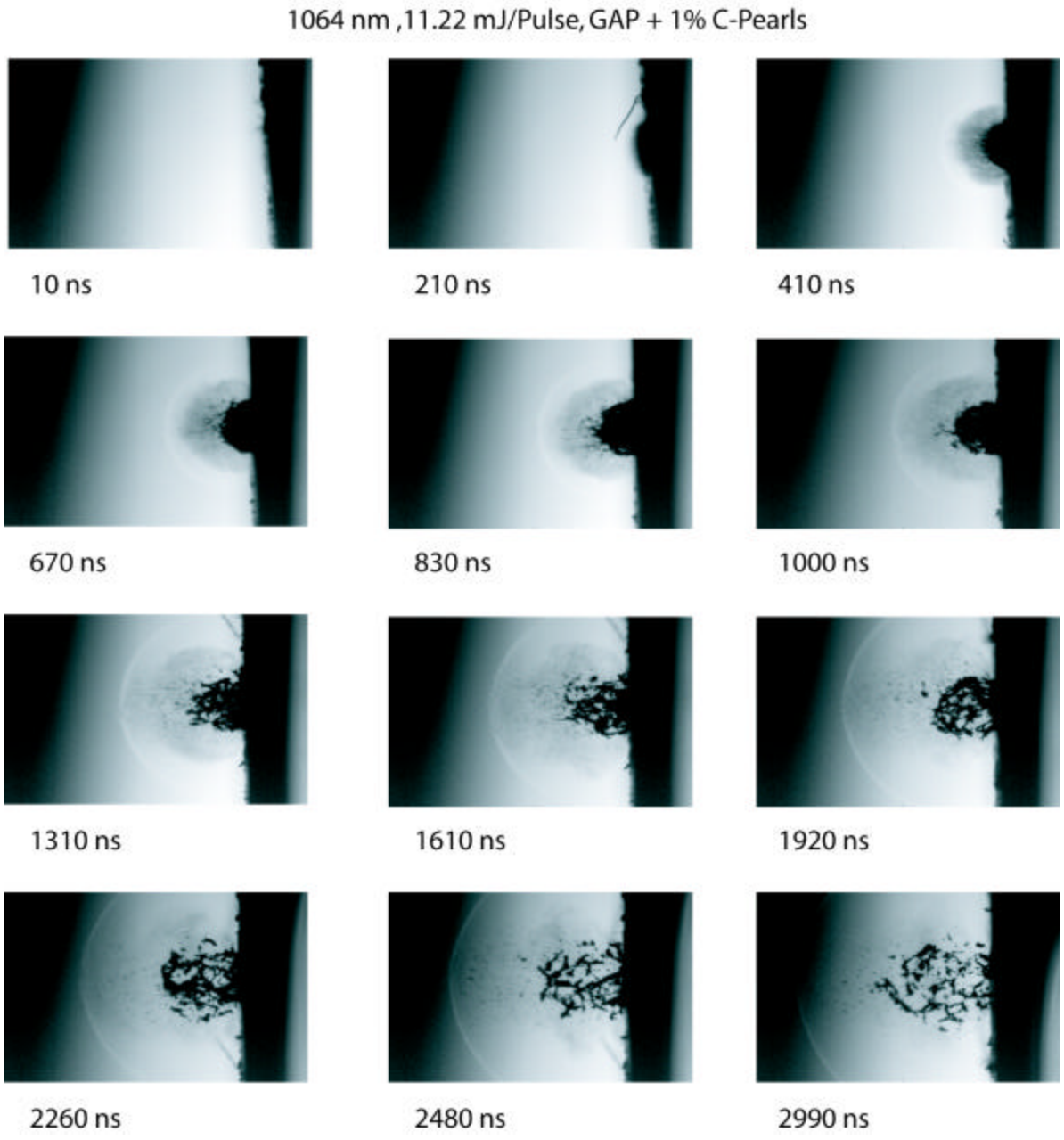

Figure 3: Comparison of the shadowgraphy images of GAP for different time delays; front side irradiation (image size: 3.77 * 2.37 mm).

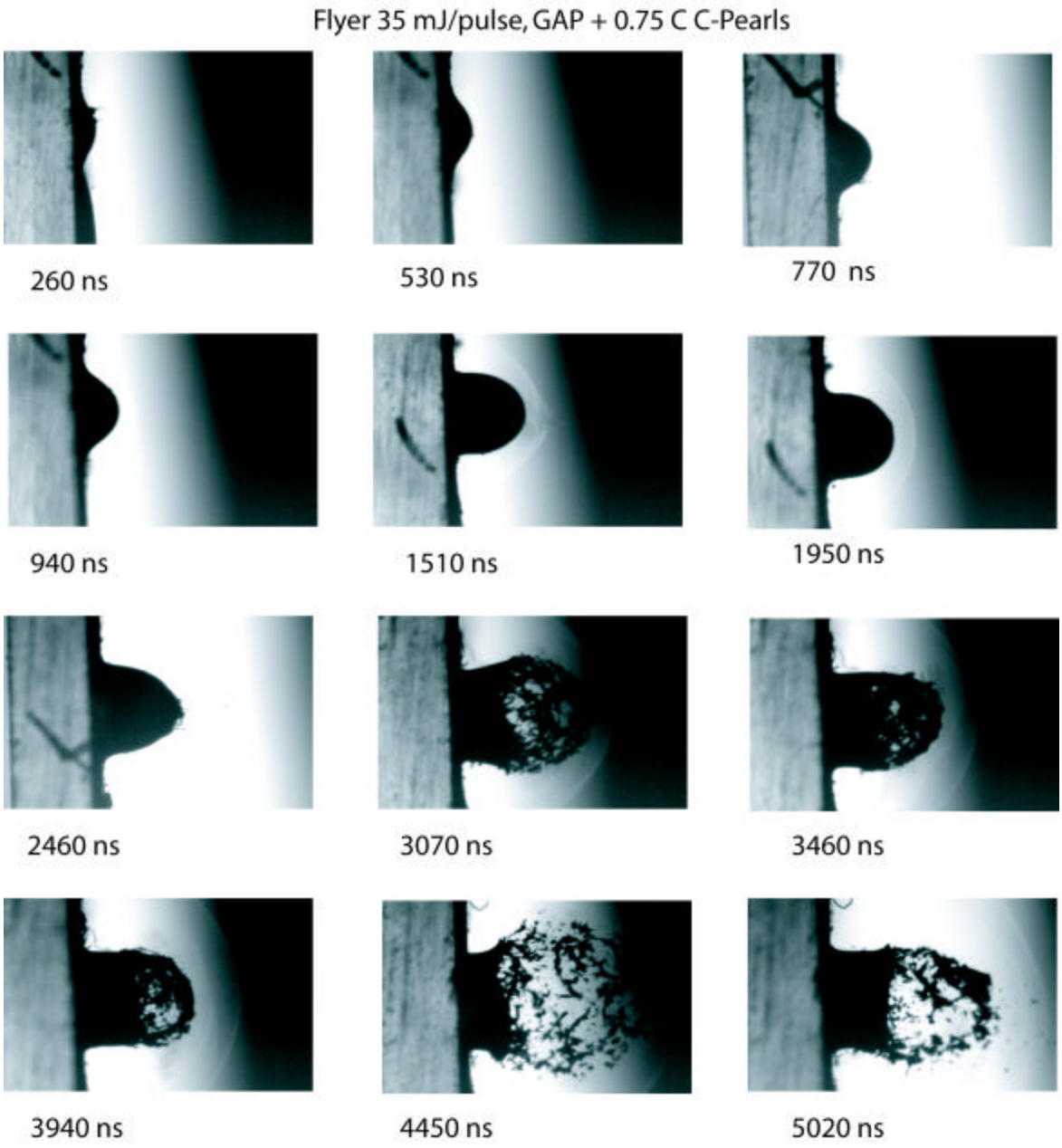

Figure 4: Comparison of the shadowgraphy images of GAP for different time delays; backside irradiation (image size: 3.77 * 2.37 mm).

The shock wave propagation was analyzed perpendicular to the polymer surface for the selected materials.

Figure 5 shows the propagation of the shock waves in air for PVC, TP and EP for irradiation at 193 nm. The two exothermic polymers, i.e. TP and EP reveal

slightly higher shockwave speeds. Whether this is due to the exothermic decomposition or other properties, e.g. different absorption coefficients has to be examined in more detail.

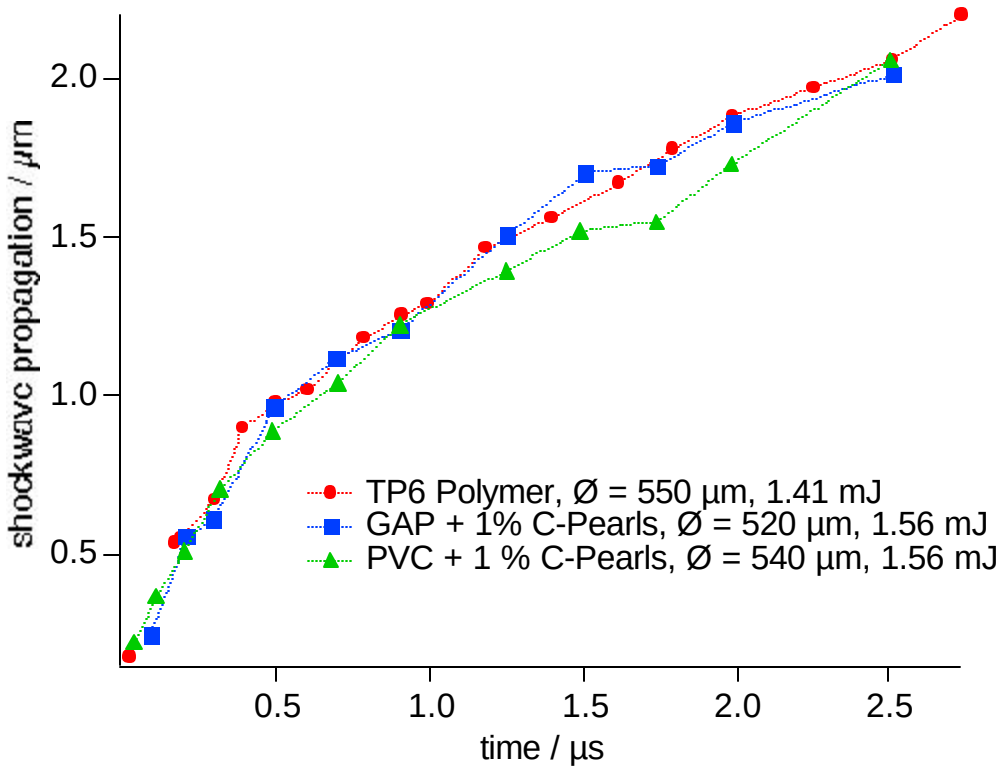

Figure 5: Comparison of the shockwave propagation after 193 nm irradiation The pulse energies for TP6 correspond to a fluence of 590 mJ cm^{-2}, for GAP to 730 mJ cm^{-2}, and for PVC to 680 mJ cm^{-2}.

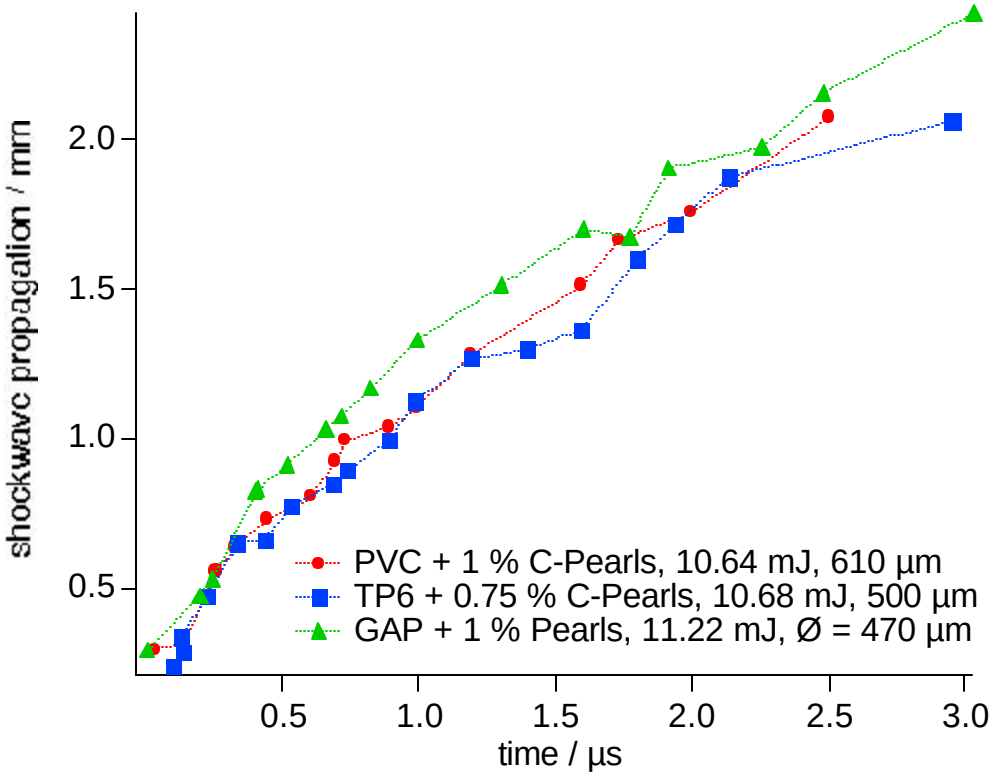

Figure 6: Comparison of the shockwave propagation after 1064 nm irradiation. The pulse energies for TP6 correspond to a fluence of 5.4 J cm^{-2}, for GAP to 6.5 J cm^{-2}, and for PVC to 3.64 J cm^{-2}.

Figure 6 shows the propagation of the shockwaves after irradiation at 1064 nm. GAP reveals the fastest shock waves, while TP and PVC seems to be quite similar. This suggests that the shock wave measurements may be correlated with the thrust experiments. It is noteworthy to mention that for experiments with 1064 nm irradiation much higher pulse energies were applied than for 193 nm irradiation. A comparison of the shock wave speeds for GAP and the two irradiation wavelengths is shown in Figure 7. The shock wave speed for GAP irradiated at 1064 nm is very similar to shock wave speeds obtained for 193 nm irradiation but with pulse energies of 1.56 mJ $pulse^{-1}$ (compared to the 11.22 mJ $pulse^{-1}$ for 1064 nm). The third curve shows clearly that the shock wave speed increases with increasing laser energy. Another important factor is probably the amount of gaseous products which support the shock wave speed. In the case of

193 nm irradiation only gaseous products are detected, which are supporting the shock wave (larger volume than solid products).

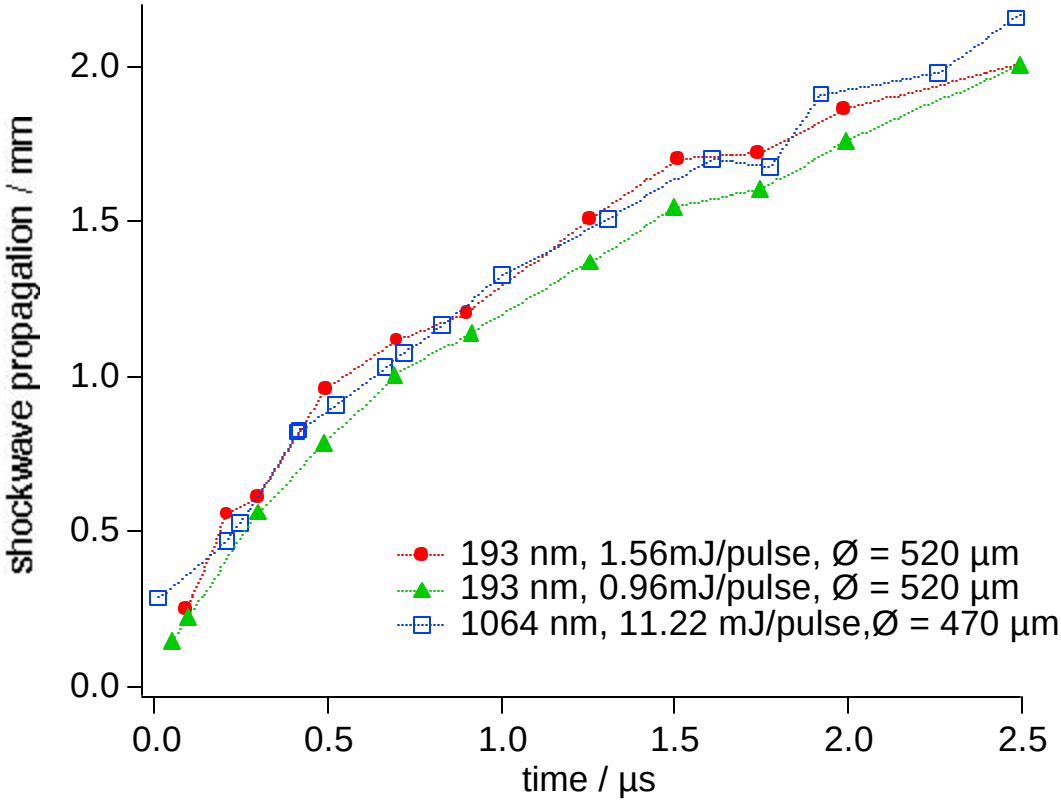

Figure 7: Comparison of the shockwave propagation of GAP with 1% of C with different irradiation wavelengths. The pulse energies for GAP correspond to 735 mJ cm^{-2} (for the 1.56 mJ $pulse^{-1}$), to o 450 mJ cm^{-2} (for the 0.96 mJ $pulse^{-1}$), and to 6.32 J cm^{-2} (for the 11.22 mJ $pulse^{-1}$ at 1064 nm).

All the above described experiments were performed with laser fluences below the threshold of plasma formation, while the plasma formation was analyzed with a time-resolved emission spectroscopy setup. In Figure 8 the emission spectra in the range of 190 to 550 nm is shown for a delay time (between the irradiation laser and the recording of the spectra) of 2 µs with an integration time of 1 µs (after the disappearance of the Bremsstrahlung) for GAP doped with carbon. We assigned tentatively several peaks, which are quite common during ablation of polymers.

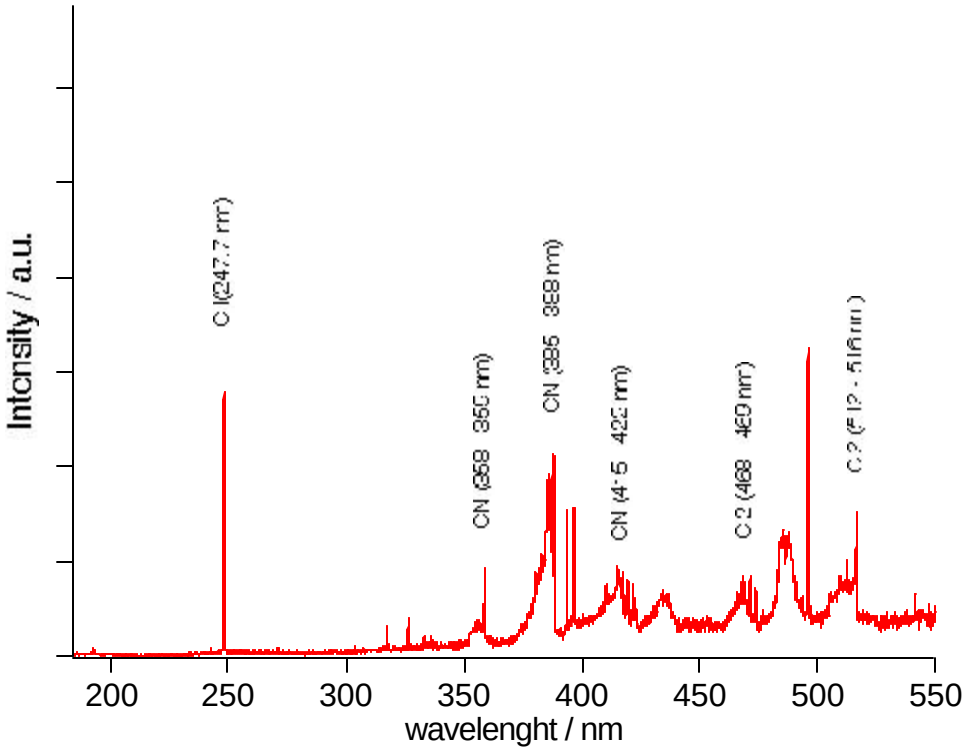

Figure 8: GAP + 0.75 % C-Pearls, 650 µm Ø, 150 mJ, delay 2 µs, integration time 1µs. The corresponding fluence is 45.2 J cm^{-2}.

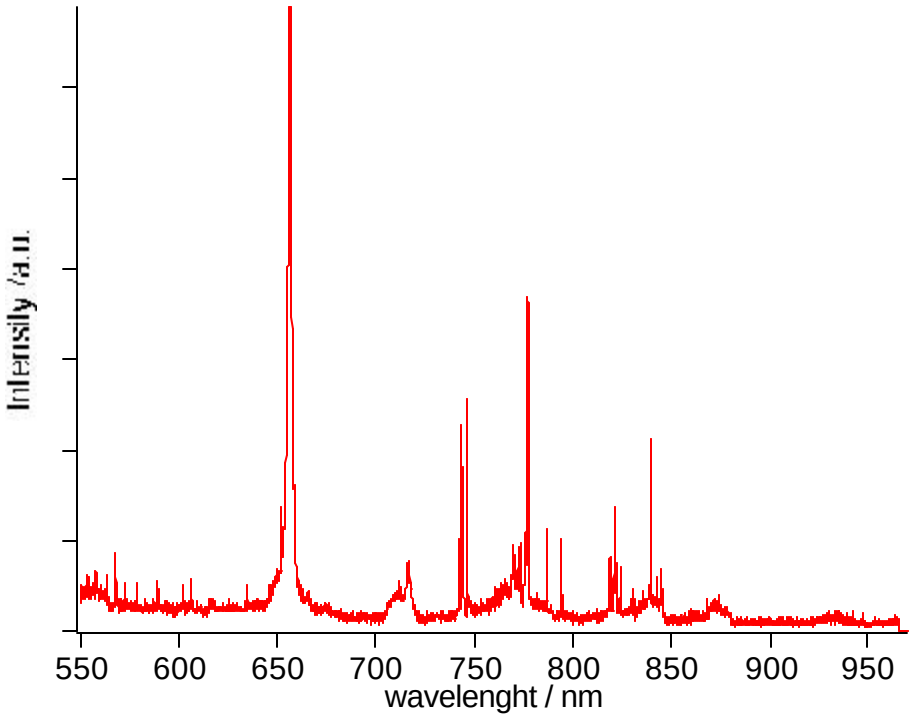

Figure 9: GAP + 0.75 % C-Pearls, 650 µm Ø, 150 mJ, delay 2 µs, integration time 1µs. The corresponding fluence is 45.2 J cm^{-2}.

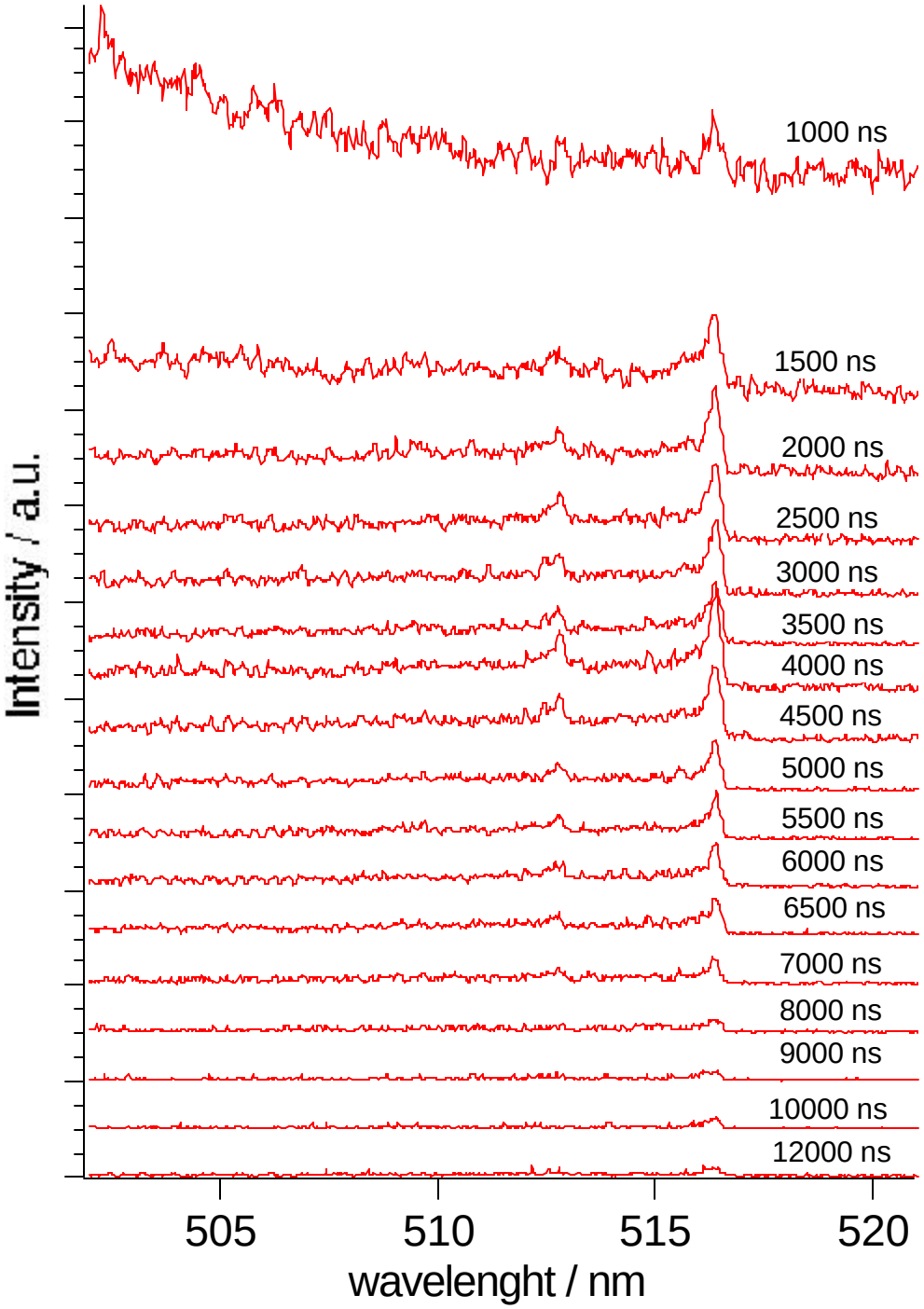

Figure 10: GAP + 0.75 % C-Pearls, 650 µm Ø, 150 mJ, variable delay, integration time 0.5 µs. The corresponding fluence is 45.2 J cm^{-2}.

In Figure 9 the second part of the emission spectra is shown (550 to 970 nm), but we have not yet assigned any peaks in this area. The evolution of two selected peaks, i.e. a peak assigned to the C_2 Swan system at 512-516 nm and a peak

assigned to the CN violet system at 385-388 nm, are shown in Figure 10 and 11, respectively. The more detailed analysis is shown in Figures 12 and 13 where the normalized peak area and corresponding background (Bremsstrahlung?) are plotted. The background and peak intensity ratios are indicated in the figures, while the ratio between the CN and C_2 band is roughly 1.54. The data points of the C_2 band (516 nm) reveal a much higher scattering, probably due to the much higher background intensity. A very similar behavior is observed for both peaks, i.e. a fast decay of the background (to about 10 % in about 2 μs) and an increase of the C_2 and CN peak to reach a maximum after around 2-2.5 μs, followed by a slow decay.

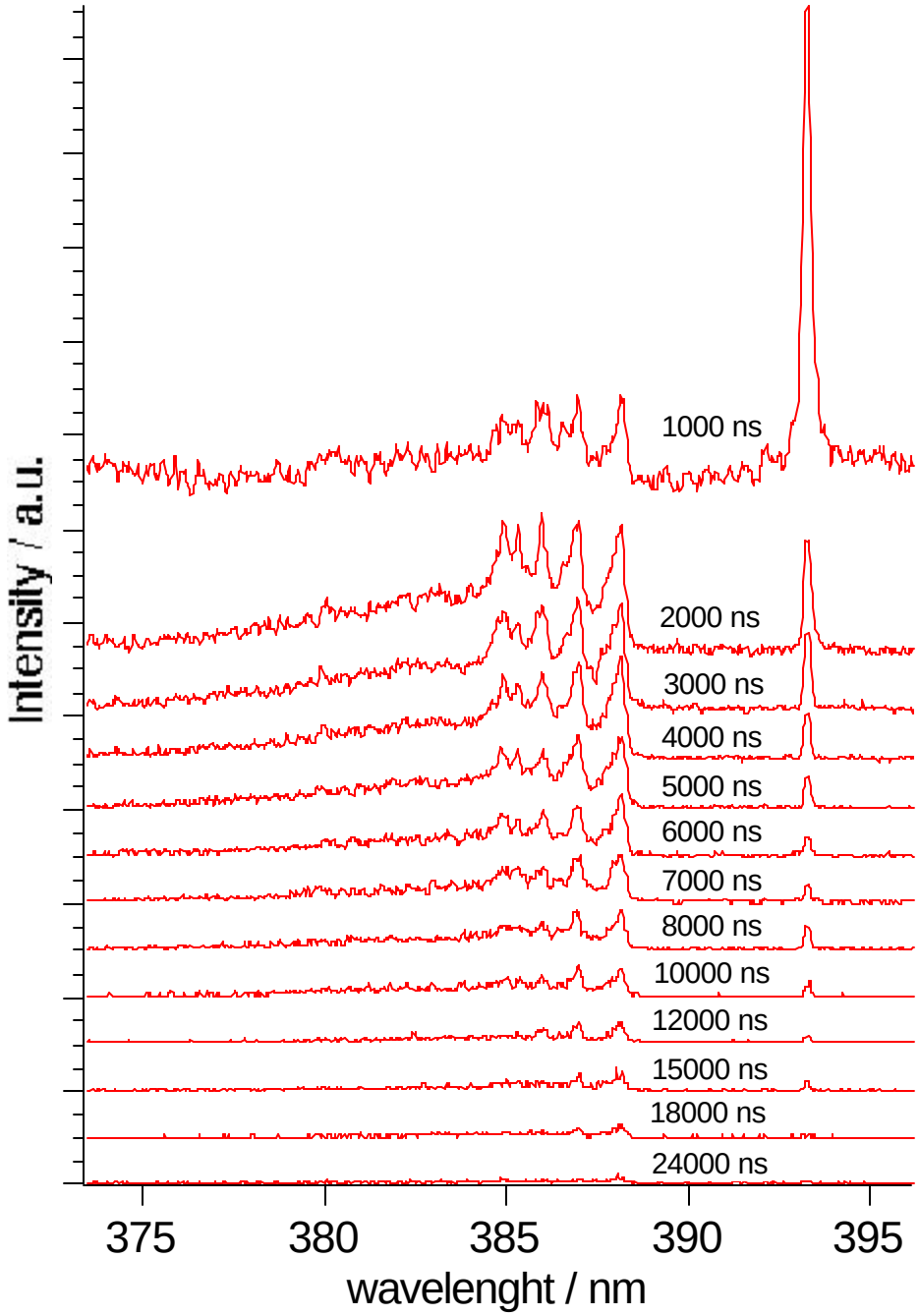

Figure 11: GAP + 0.75 % C-Pearls, 650 µm Ø, 150 mJ, variable delay, integration time 0.5 µs. The corresponding fluence is 45.2 J cm^{-2}.

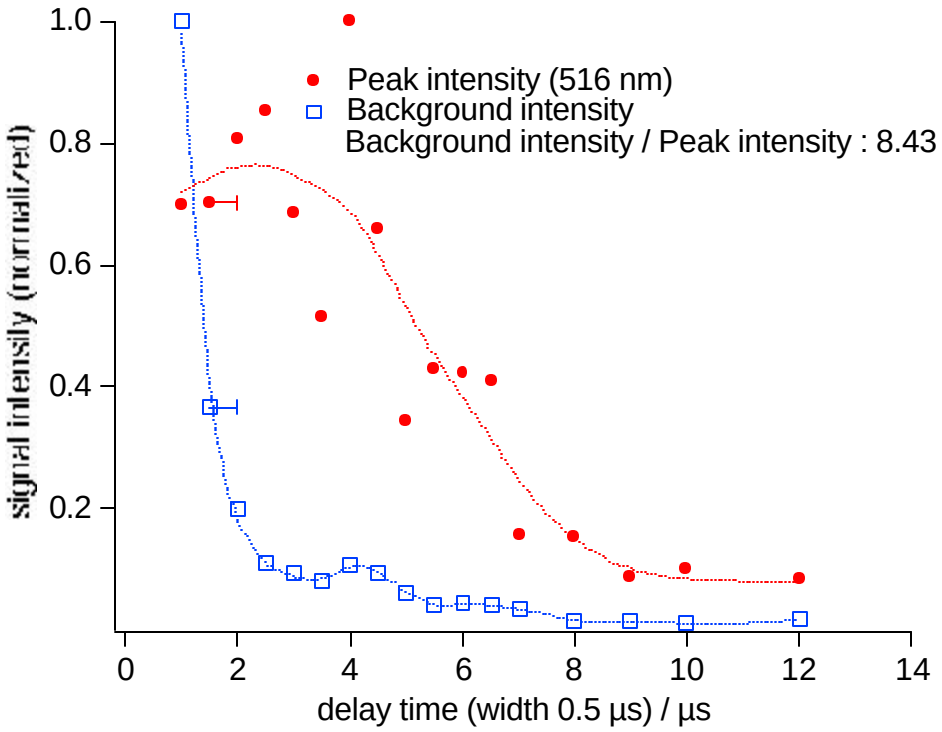

Figure 12: GAP + 0.75 % C-Pearls, 650 µm Ø, 150 mJ, variable delay, integration time 0.5 µs. Spline curves added to guide the eyes. The corresponding fluence is 45.2 J cm^{-2}.

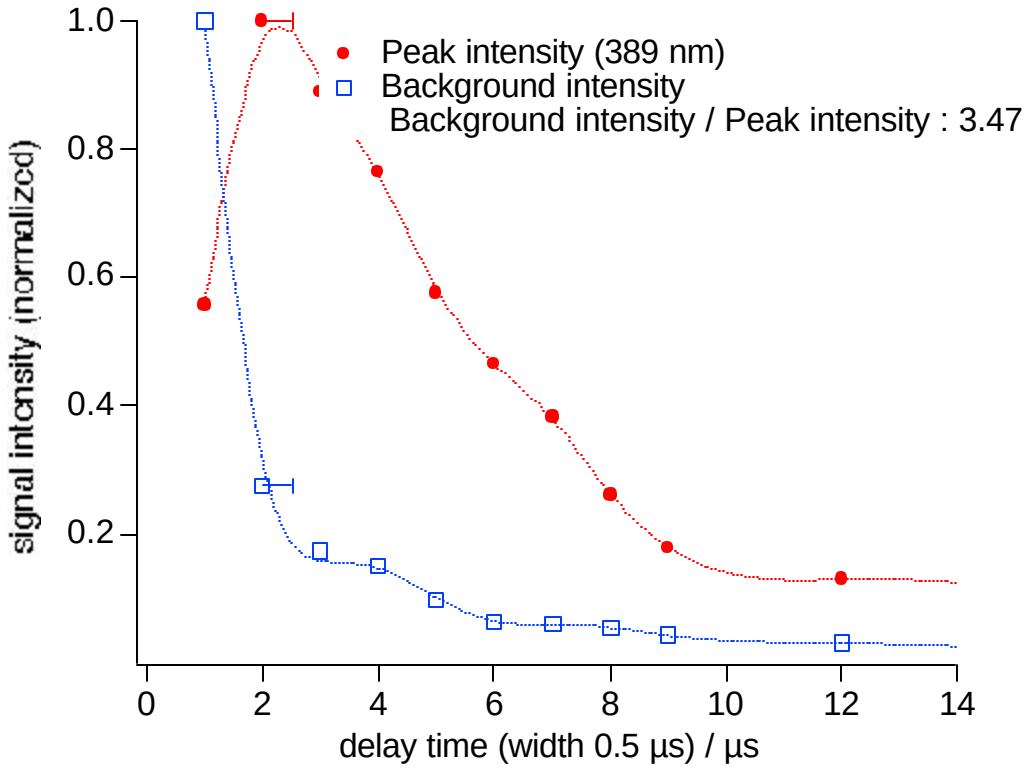

Figure 13: GAP + 0.75 % C-Pearls, 650 µm Ø, 150 mJ, variable delay, integration time 0.5 µs. Spline curves added to guide the eyes. The corresponding fluence is 45.2 J cm^{-2}.

Summary II

The above described experiments showed clearly that in the case of irradiation of the polymers with fluences below the threshold of plasma formation, the irradiation wavelengths and material are important factors. Higher shock wave speeds are obtained at the shorter irradiation wavelength (193 nm), probably due to the shorter absorption length and the larger amount of gaseous fragments. The shock wave speeds of the different materials seem to follow the same order than determined in thrust experiments (by Claude Phipps), with GAP as the best performer. The time-resolved emission spectroscopy suggests that future measurements can be used to analyze the plasma properties in more detail.

Results III: Shadowgraphy, Ablation and Emission-Spectroscopy

Therefore the analysis of the shock waves and the evaluation of the shadowgraphy images of the three selected polymers was continued. The classical shadowgraphy setup was applied for these measurements, due to the better image quality and easier evaluation procedure. The Mach-Zehnder setup is in principle more powerful, as it allows also a quantitative analysis of the changes of the index of refraction. For this analysis it is necessary to perform an inverse Abel transformation, which we could not yet implement in our analysis routine. The resulting data will then allow determining electron densities in the plasma.

We continued with the experiments on the three selected polymers, i.e. PVC, GAP and TP (structural units shown in Scheme 2).

The images from the shadowgraphy experiments of PVC, especially for carbon doped PVC and an irradiation wavelength of 1064 nm are shown in Figure 14.

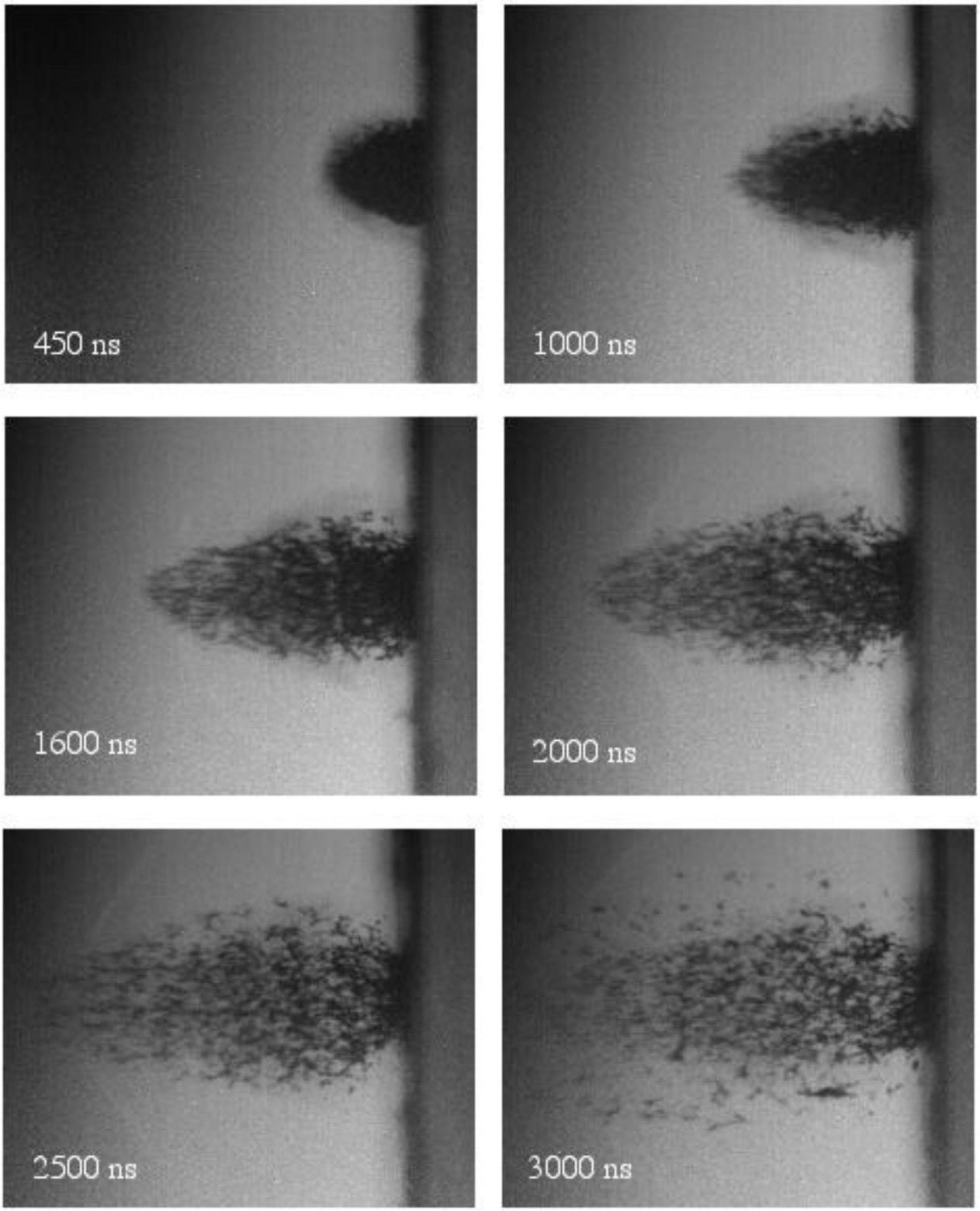

Figure 14: Shadowgraphy images of the ablation of PVC doped with carbon. Irradiation wavelength: 1064 nm with10.6 mJ per pulse (3.64 J cm^{-2}).

The images of the PVC ablation show a very interesting behavior. The product ejection seems to be more directional, resulting in an overtaking of the shock wave (after 2 µs) front by the products (to our knowledge not observed before). This effect is only observed for higher irradiation fluences (e.g. not observed for a

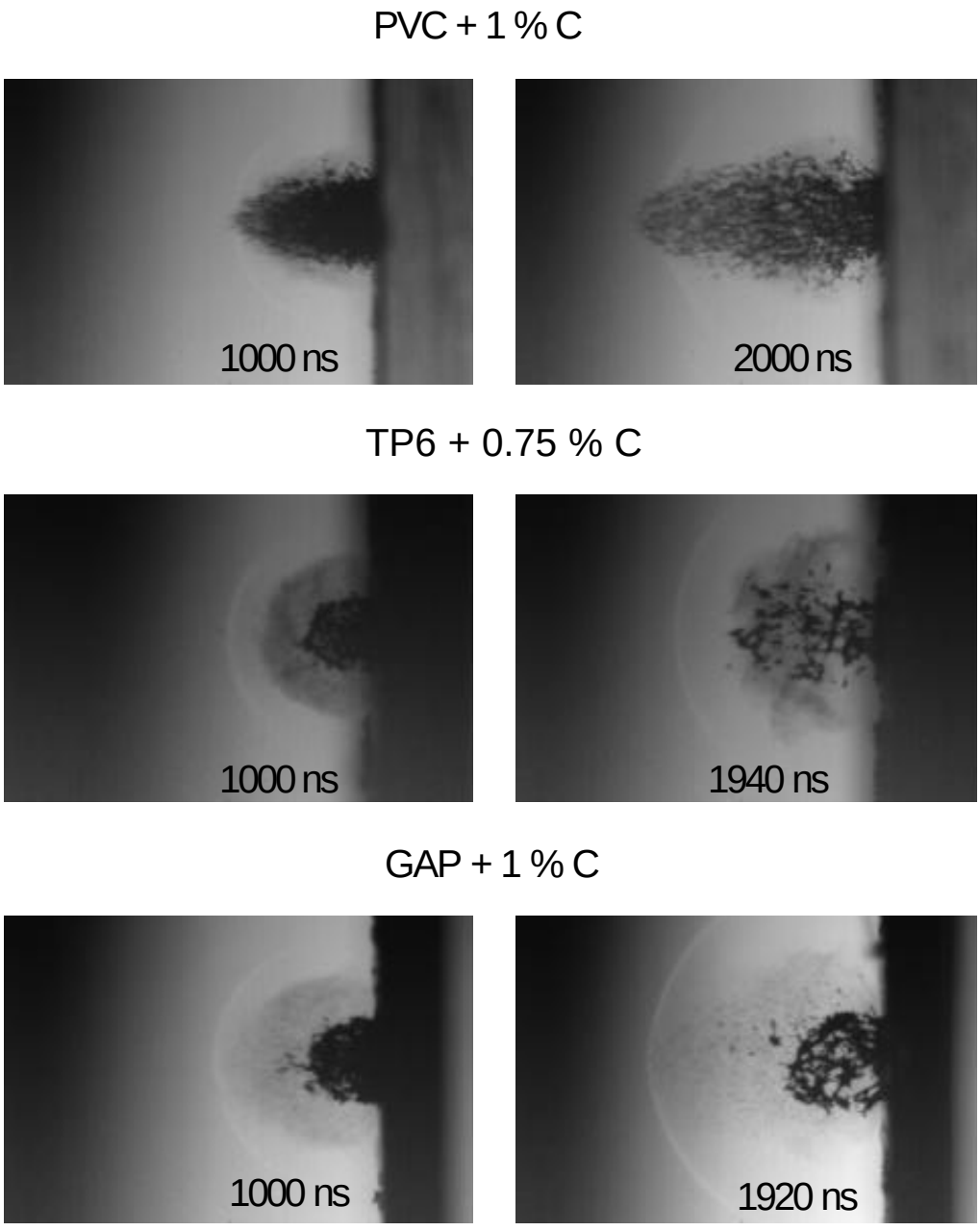

Figure 15: Comparison of shadowgraphy images for the three polymers (1064 nm irradiation). Fluence from top: 3.64, 5.44, and 6.47 J cm^{-2}.

fluence of 1.94 J cm^{-2}) and only for PVC doped with carbon and an irradiation wavelength of 1064 nm. The reason for this behavior is not clear right now, but may be related to a large amount of solid products that are ejected during 1064 nm irradiation of PVC. The amount of solid fragments is higher for PVC compared to TP and GAP, as shown in Figure 15.

The images (after 1 and ~ 2 μs) reveal that in the case of PVC a large amount of particles is ejected, with a directional shape (bullet like) of the ablation products. For the irradiation of TP6 and GAP a quite different behavior is observed, i.e. the ablation products seem to consist of two fractions: one with smaller fragments or may be mainly gaseous products, and a second fraction with larger fragments. The shape of the ablation products is more hemispherical and with slight mushroom form in the later stages (especially for TP6). These shapes are consistent with the normally observed shapes during ablation. Other parameter that may influence the ablation characteristics will be discussed below.

The clear difference between the larger fragments and the gaseous products and the relatively sharp contours of the product allows analyzing the shadowgraphy

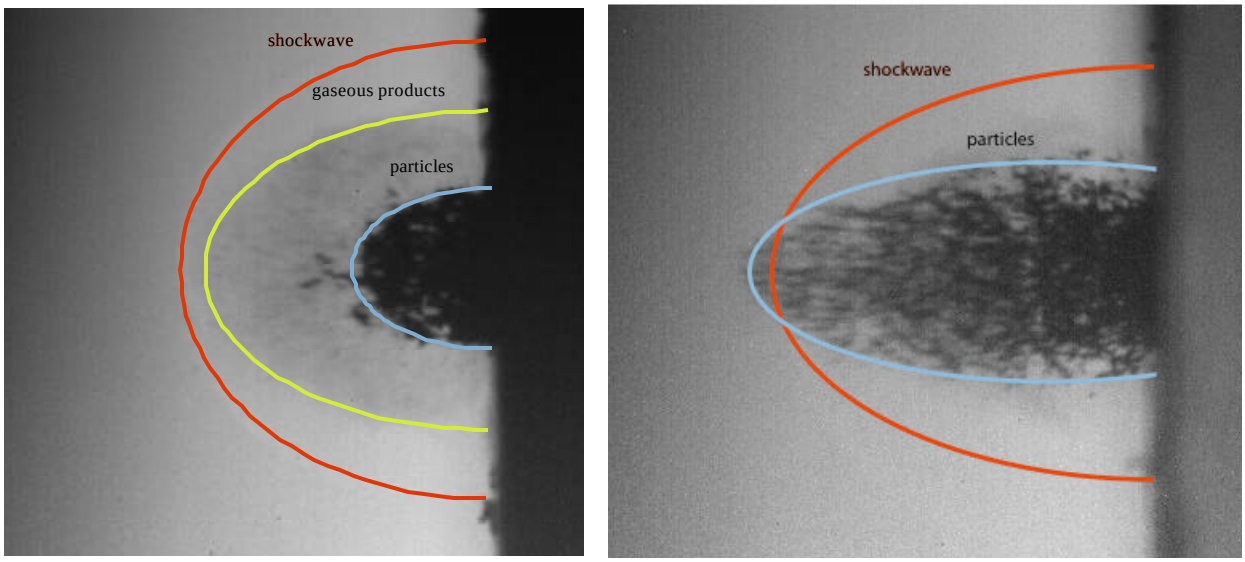

Figure 16: Definition of shockwave, gaseous products and particles for GAP (left) and PVC (right). Irradiation at 1064 nm.

pictures in more detail. We analyzed now in addition to the shock wave velocities

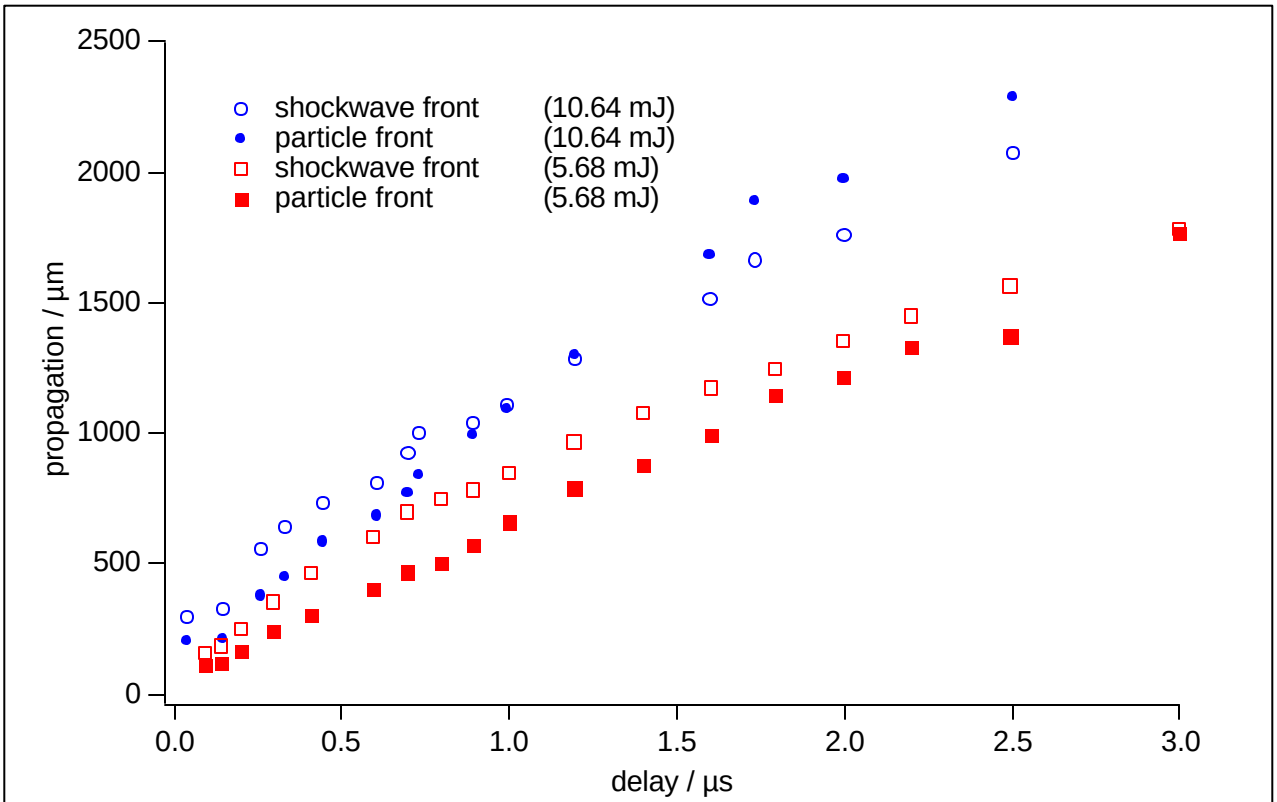

Figure 17: Analysis of the shock wave and particle front propagation for PVC doped with 1 % of carbon. Irradiation at 1064 nm, with 3.64 J cm^{-2} (10.64 mJ) and 1.94 J cm^{-2} (5.68 mJ).

the velocity of the "solid" and "gaseous" product fronts. The definitions of these two fronts are depicted for GAP and PVC in Figure 16.

The analysis of the particle front and shock wave expansion is shown for PVC in Figure 17 for two fluences (10.64 mJ corresponds to 3.64 J cm^{-2-}, while 5.68 mJ corresponds to 1.94 J cm^{-2}). For the higher fluences it is clearly visible that the particle front overtakes the shock wave around 1 µs, while at the lower fluence the particle front may only reach the shock wave after 3 µs.

In Figure 18 the analysis for GAP is shown, where the shock wave front is neither reached by the gaseous product front nor the particles front. This is even more remarkable, because a much higher fluence has been applied, i.e. 6.47 J cm^{-2}. The quite different fluences for the same laser pulse energy are caused by different sizes of the ablation craters for a given fluence (discussed in detail later, but this was not mentioned in the previous report, where we assumed that the

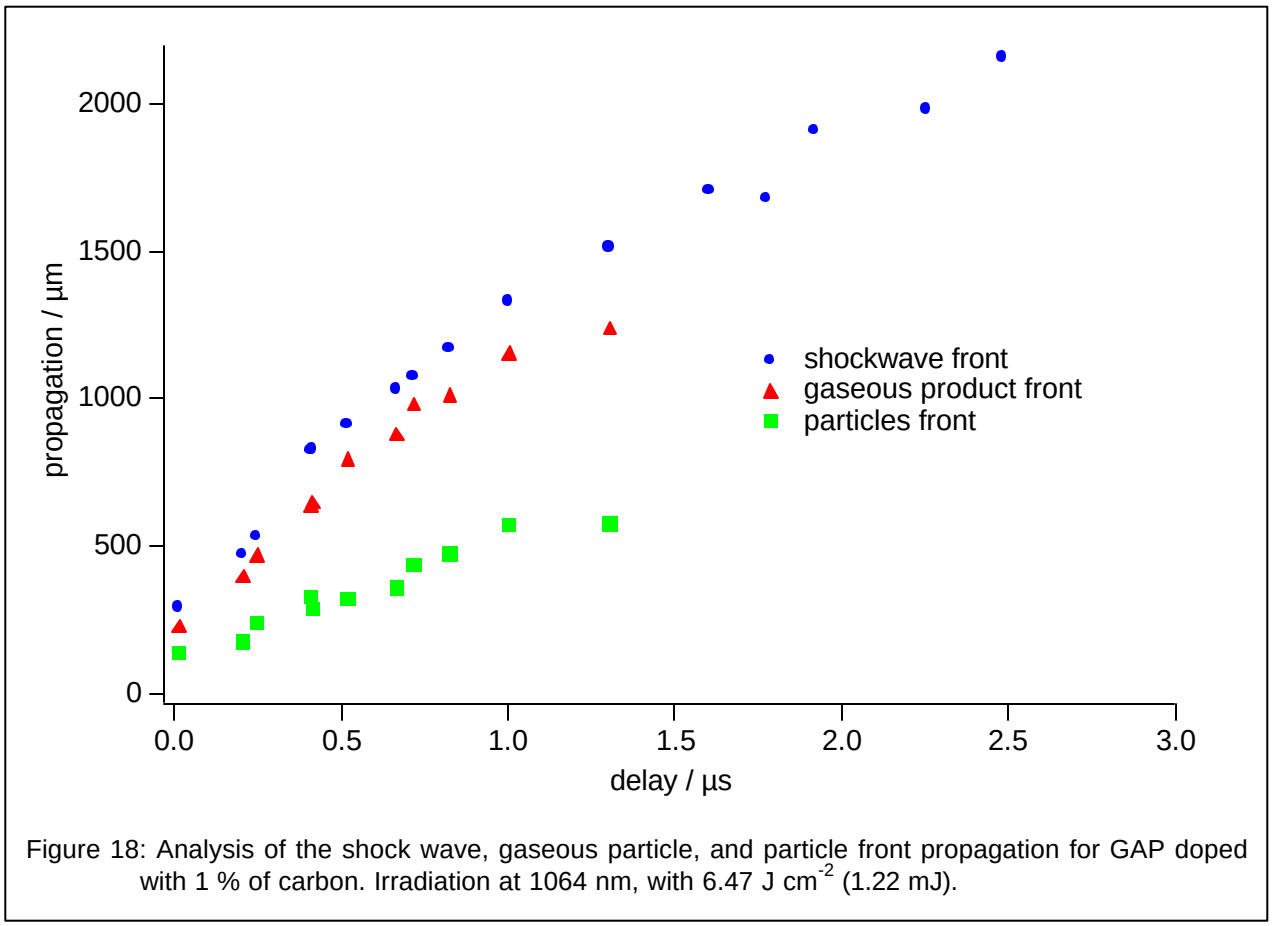

Figure 18: Analysis of the shock wave, gaseous particle, and particle front propagation for GAP doped with 1 % of carbon. Irradiation at 1064 nm, with 6.47 J cm^{-2} (1.22 mJ).

same pulse energy will correspond to the same fluence. We measured now the ablation crater and realized this important fact).

A direct comparison of the shockwave or product velocities between the two polymers is unfortunately not possible, due to the different laser fluences.

The very different fluences are, as mentioned above, caused by different diameters of the ablation craters for the different polymers. The change of ablation diameter can be explained by the Gaussian shape (energy distribution over the beam area) of the 1064 nm laser pulse, assuming that the threshold fluences (the fluence were ablation starts) are different. In the case of a lower ablation threshold a larger part of the Gaussian beam causes ablation, while for a higher threshold fluence only a smaller part of the beam has enough energy to cause ablation. This can be confirmed by analyzing the ablation rate per pulse for various fluences, as shown for GAP and PVC (both doped with carbon) for 1064

nm irradiation in Figure 19. Polymer ablation is normally characterized according to the following empirical equation (1)

$$d(F) = \frac{1}{\alpha_{eff}} \ln\left(\frac{F}{F_{th}}\right) \qquad (1)$$

where d (F) is the ablation rate (ablation depth per pulse), α_{eff} is the effective absorption coefficient and F_{th} is the threshold fluence. The plot of the ablation

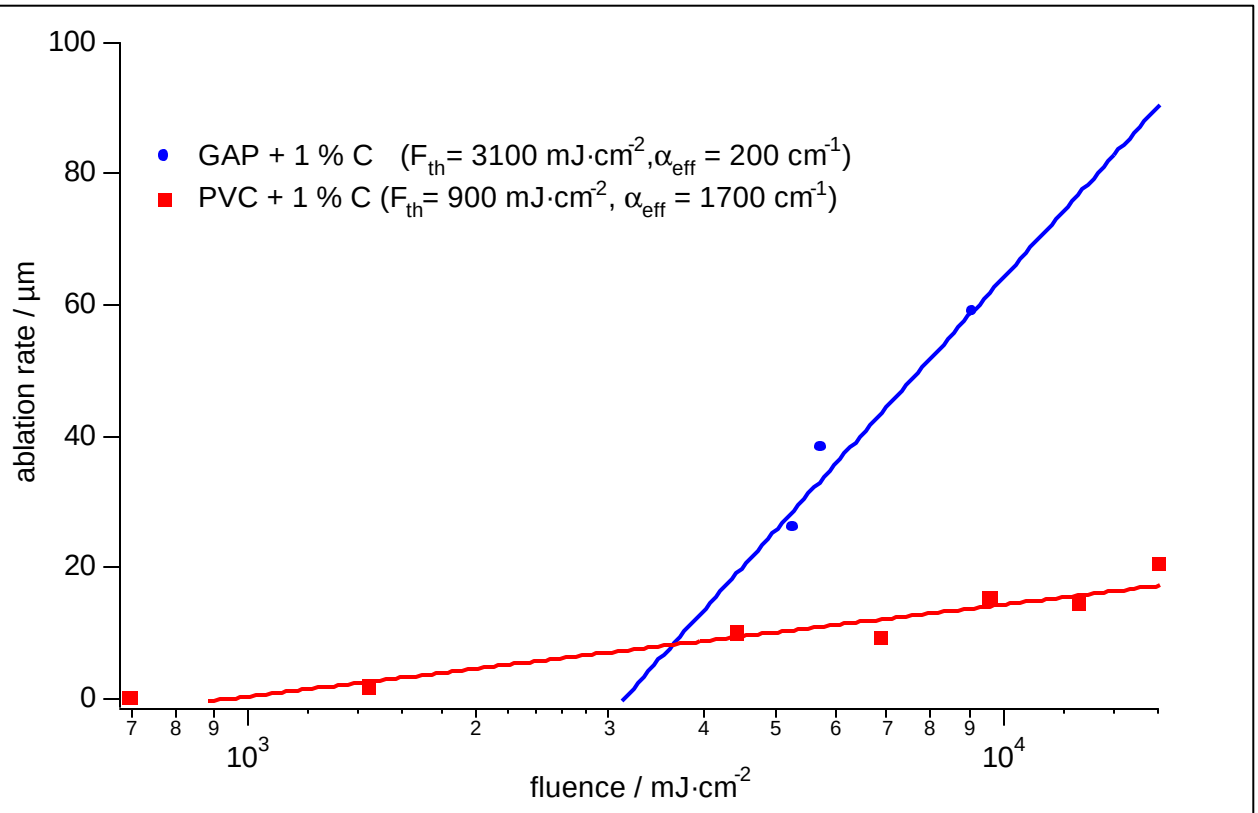

Figure 19: Ablation rates for carbon doped GAP and PVC. Irradiation at 1064 nm.

rate versus the logarithm of the fluence allows calculating α_{eff} and F_{th}, which are included in Figure 19.

The threshold fluences are as expected very different, i.e. 3100 mJ cm^{-2} for GAP and 900 mJ cm^{-2} for PVC. GAP reveals also a much higher ablation rate (indicated also by the smaller effective absorption coefficient). These pronounced differences are totally unexpected, as both polymers have a similar absorption

coefficient (discussed below, but both are transparent in their pure form, and are doped with the same amount of carbon, i.e. 1%). A first fast literature search about the thermal properties was not really successful, because the variations in data, especially for PVC are quite large. The data which were found are listed below in Table 1.

Table 1: Comparison of thermal properties of GAP and PVC

Data	**GAP**	**PVC**
Decomposition temperature [^{0} C]	215 –240	start at 80, but main part between 220-255
Activation energy [kJ mol^{-1}]	164.85	120.2-228.9
Pre-exponential factor	6.31 * 10^{13}	1.18 * 10^{12} – 1.0 8 10^{16}
Heat of reaction [J g^{-1}]	2.365 (EXOTHERMIC]	39.4 ?????? [ENDOTHERMIC]??

It will be absolutely necessary to control and evaluate these data further. The heat of reactions seems to be at least questionable.

Both polymers reveal in principle a similar decomposition pathway, i.e. they decompose in several steps: first elimination of N_2 for GAP and HCl for PVC, followed by the decomposition of the remaining structure. The table above suggests that the decomposition will start in a similar temperature range (of course assuming that slow heating, i.e. 5 K s^{-1} results in the same data as laser heating with heating rates of up to 10^9 K s^{-1}, which may be questionable). An estimate about the energy balances suggests also that direct “photon-induced decomposition” (with as single photon) is not possible:

Photon energy (1064 nm): 1.16 eV, energy of the C-Cl bond: ˜ 3.5 eV, energy of the N-N bond: 1.7 eV (minimum value for the azide group).

The most plausible reaction pathway is as follows: the carbon absorbs the laser energy and converts the photon energy into heat, causing the decomposition of the polymer in the vicinity of the carbon dopant. In the case of irradiation at 193

nm a quite different behavior can be expected. The polymers are absorbing the irradiation wavelength directly, and the photon energy (6.59 eV) is more than enough to break all bonds in the polymers directly. GAP has a much higher absorption coefficient (shown below) than PVC at 193 nm, which results in a deposition of the laser energy in a smaller volume element. This normally results

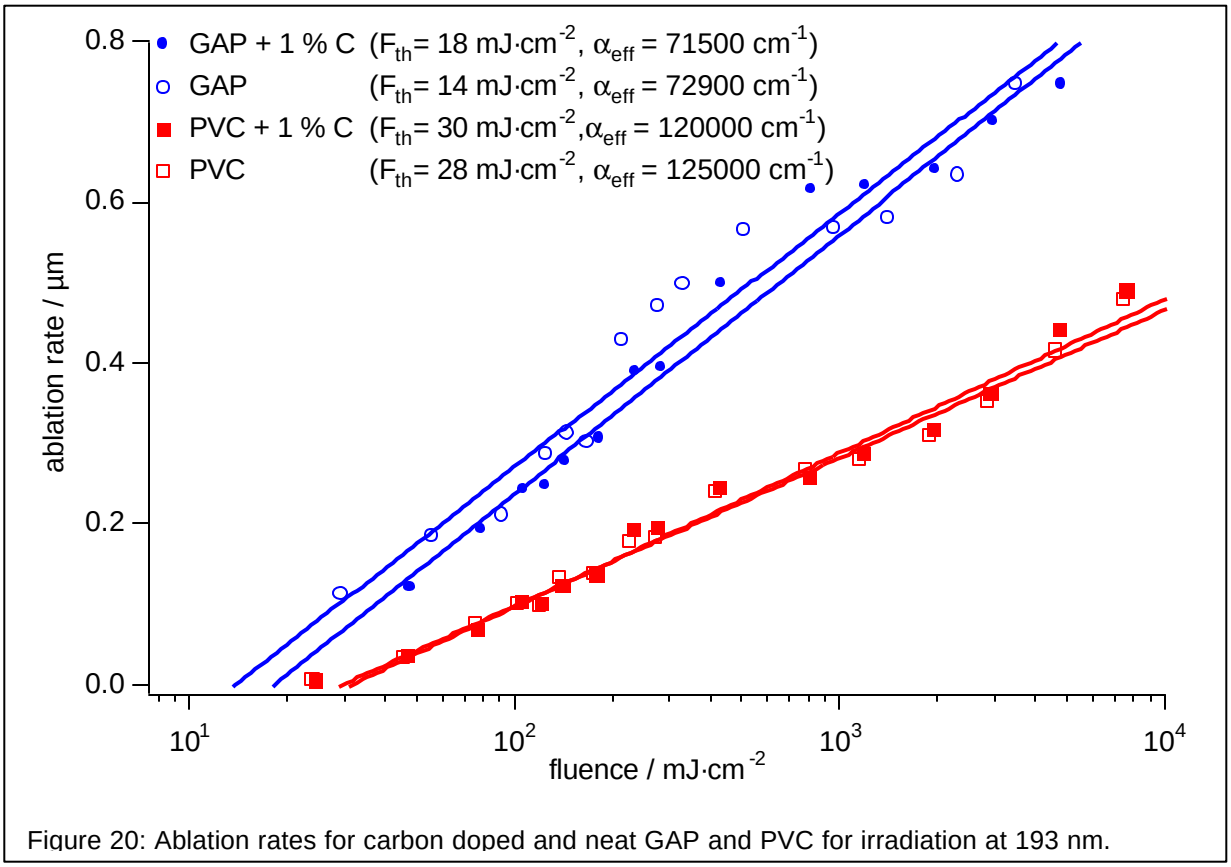

Figure 20: Ablation rates for carbon doped and neat GAP and PVC for irradiation at 193 nm.

for UV ablation of polymers in lower ablation thresholds.

The comparisons of the ablation rates for PVC and GAP for 193 nm irradiation with and without carbon dopant are shown in Figure 20.

GAP reveal as expected the lower ablation threshold, but also higher ablation rates, which is probably due to decomposition of the polymer during the laser pulse (resulting in larger ablation rates, due to “pseudo” higher laser penetration depths). This behavior is also observed for TP or other polymers that decompose photochemically during the laser pulse. The larger effective absorption coefficient of PVC (compared to the linear absorption coefficient, shown below), suggest that absorbing species are created during the laser pulse, which lower the laser

penetration depths. The carbon doped samples have slightly higher thresholds, probably due to the higher threshold of pure carbon (compared to the pure polymer).

The above mentioned linear absorption coefficients of all polymers (including TP)

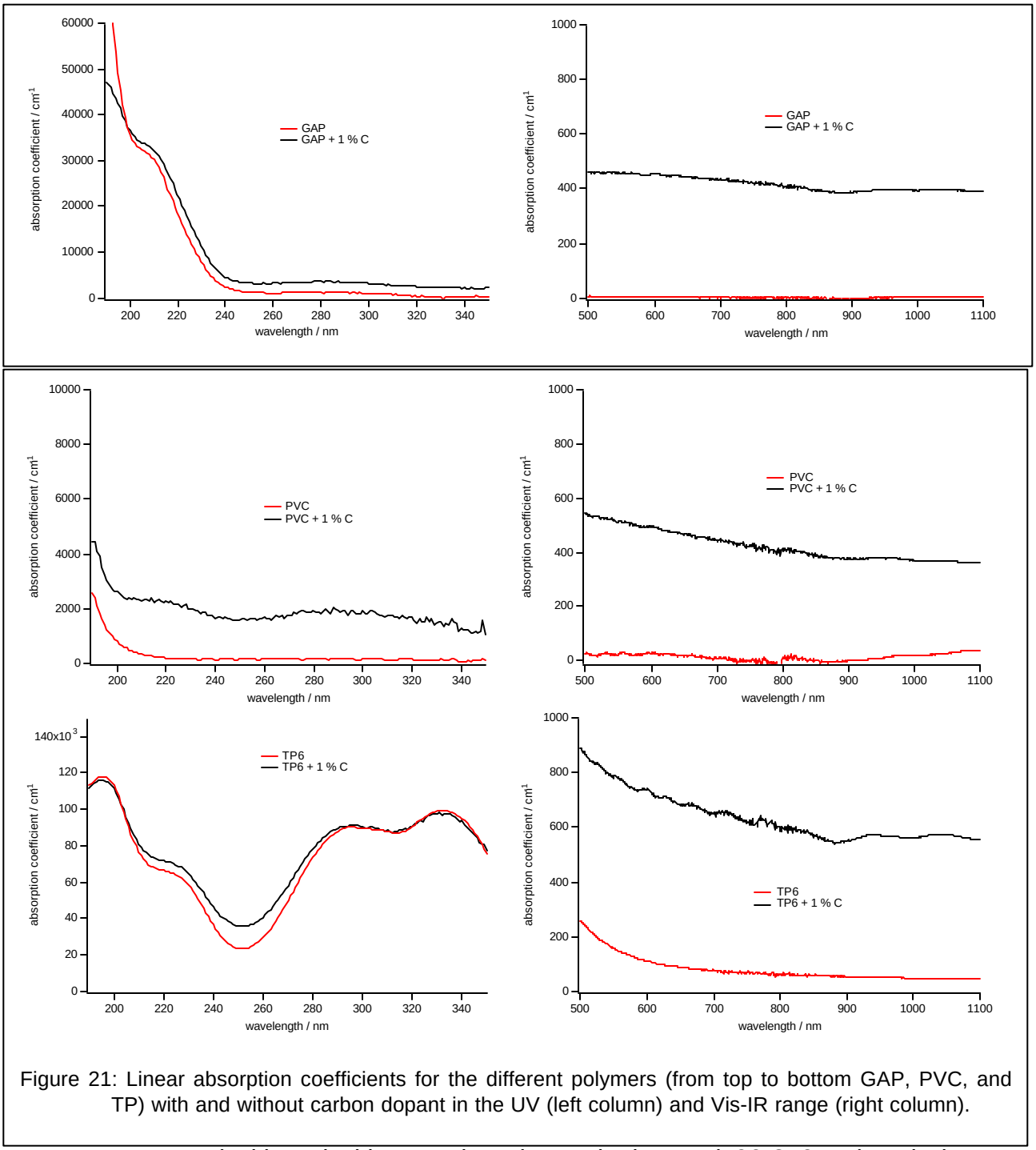

Figure 21: Linear absorption coefficients for the different polymers (from top to bottom GAP, PVC, and TP) with and without carbon dopant in the UV (left column) and Vis-IR range (right column).

were measured with and without carbon dopant in the UV (190-350 nm) and Vis-

IR range (500-1100 nm) for thin polymer films on glass or quartz substrates. The method utilizes a standard UV-Vis-NIR spectrometer, where the absorption of the films is measured, and a profilometer, where the thicknesses of the films are determined. The correlation of these two data sets gives the linear absorption coefficients as a function of wavelengths (shown in Figure 21).

The absorption coefficient spectra reveal the already discussed data:

- All polymers absorb at 193 nm in the order TP, GAP, and PVC.
- Carbon doping increases the absorption over the whole wavelength range.
- All polymers are transparent in the IR.
- Carbon induces a small absorption (due to the low dopant concentration) at 1064 nm.
- The values of the absorption coefficients (at 1064 nm) are consistent for carbon doped PVC and GAP, but deviate for TP (reason not clear).

An increase of the laser fluence results in the creation of a plasma that can be used for a further analysis of the ablation process. The plasma range is of course also the most interesting part for an application of these polymers in laser plasma thrusters.

The emission spectra for GAP+C and the temporal evolution of various bands after irradiation with 1064 nm (fluence: 45.2 J cm^{-2}) were shown in the previous report. A detailed analysis of the bands allows calculating plasma temperatures and electron densities (Stark broadening). The analysis of the plasma temperatures is performed to test whether it is possible to correlate the plasma properties, especially temperatures, with the thrust obtained in the LPT experiments of Claude Phipps. To perform these calculations it is necessary to obtain well-resolved spectra with high signal to noise ratio, which was not the case for the spectra shown above. Therefore experiments were performed with an irradiation wavelength of 193 nm (fluence 4.65 Jcm^{-2}), where the emission spectra have sufficient quality to perform the analysis to determine the plasma temperature. The setup for 1064 nm irradiation was simultaneously improved (better optic to obtain higher fluences, and better setup geometry to optimize the

signal resolution and intensity) to perform the same experiments for 1064 nm irradiation.

The plasma temperature calculations are based on the program LIFBASE.[2] This software reproduces the spectra of diatomic molecules by calculating the intensity summation of all rovibrational levels convoluted with the instrumental line shape of the optical system. The intensities are thereby obtained using Equation 2.

$$I_{v''J''}^{v'J'} = KA_{v''J''}^{v'J'}N_{v'J'} \qquad (2)$$

K is an experimental constant depending on the optical configuration. $N_{v'J'}$ is the population in the excited state which is determined assuming a thermalized system, using a Boltzmann distribution to determine the population density. The Einstein coefficient $A_{v''J''}^{v'J'}$ was calculated according to Equation 3

$$A_{v''J''}^{v'J'} = \frac{g_e'}{g_e''}\frac{64p}{3h}\frac{S_{J''}^{J'}}{2J'+1}p_{v''J''}^{v'J'}(u_{v''J''}^{v'J'})^3 \qquad (3)$$

g_e is the electronic degeneracy which takes the state spin multiplicity into account. S is the Honl-London factor, which was used following the analytical expression by Kovacs and Earls[3,4] and the normalization following the suggestion by Whiting[5] [4]. p is the transition probability previously calculated and included in the database of the program. ν is the transition frequency.

The vibrational sequence with $\Delta v=0$ of the CN-Violet system ($B^2\Sigma \rightarrow X^2\Sigma^+$) at 385-388 nm used to simulate the emission, and by comparing the simulated spectra at different temperatures with the measured spectra, to identify the plasma temperature. The assumption that the system was in a thermalized state is not totally valid, resulting in differences between the simulation and the measured

---

[2] J. Luque and D.R. Crosley, "LIFBASE: Databse and Spectral Simulation Program (Version 1.5)", SRI International Report MO 99-009 (1999)

[3] I. Kovacs, *Rotational structure in the spectra of diatomic molecules*, Adam Hilger Ltd., London (1969)

[4] L.T. Earls, *Intensities in ${}^2P$ ® ${}^2S$ transition in diatomic molecules*, Phys. Rev. **48**, 423 (1935).

[5] E.E. Whiting, J.A. Paterson, I. Kovacs and R.W. Nicholls, *Computer checking of rotational line intensity factors for diatomic molecules,* J. Molec. Spectros. 47,84 (1973).

spectra. These difference could only be reduced when the population densities of the vibrational states was chosen manually.

An example of a measured spectrum (193 nm irradiation of GAP + C) with the simulated spectra, assuming a thermalized and non-thermalized system is shown in Figure 22. The fit of the thermalized spectrum yields a plasma temperature of 7500 K, while the simulation for the non-thermalized spectrum yields 6700 K with

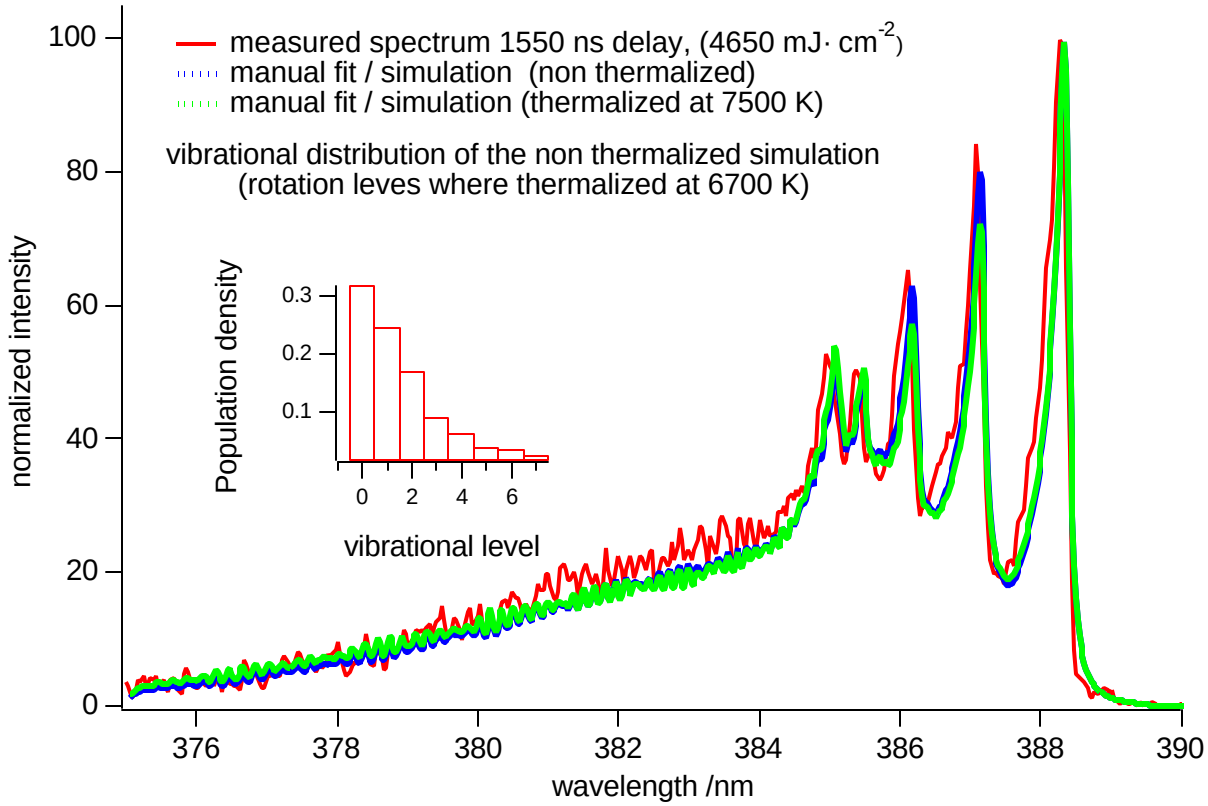

Figure 22: Emission spectra of GAP+C in the region of the CN violet system with added simulation of the spectrum assuming a thermalized and non-thermalized system. The inset shows the population density of the vibrational levels for the non-thermalized simulation.

a population density of the vibrational levels as shown in the insert of Figure 22. The evolution of the plasma temperature with time is shown in Figure 23 for various fluences. For all fluences a fast decay of the plasma temperature is observed for the first 5 μs followed by a slower decay over the next 15 μs. The large variations of the temperatures at later times is due to the decreasing intensity of the emission lines, which results in larger deviations during the simulation.

Summary III

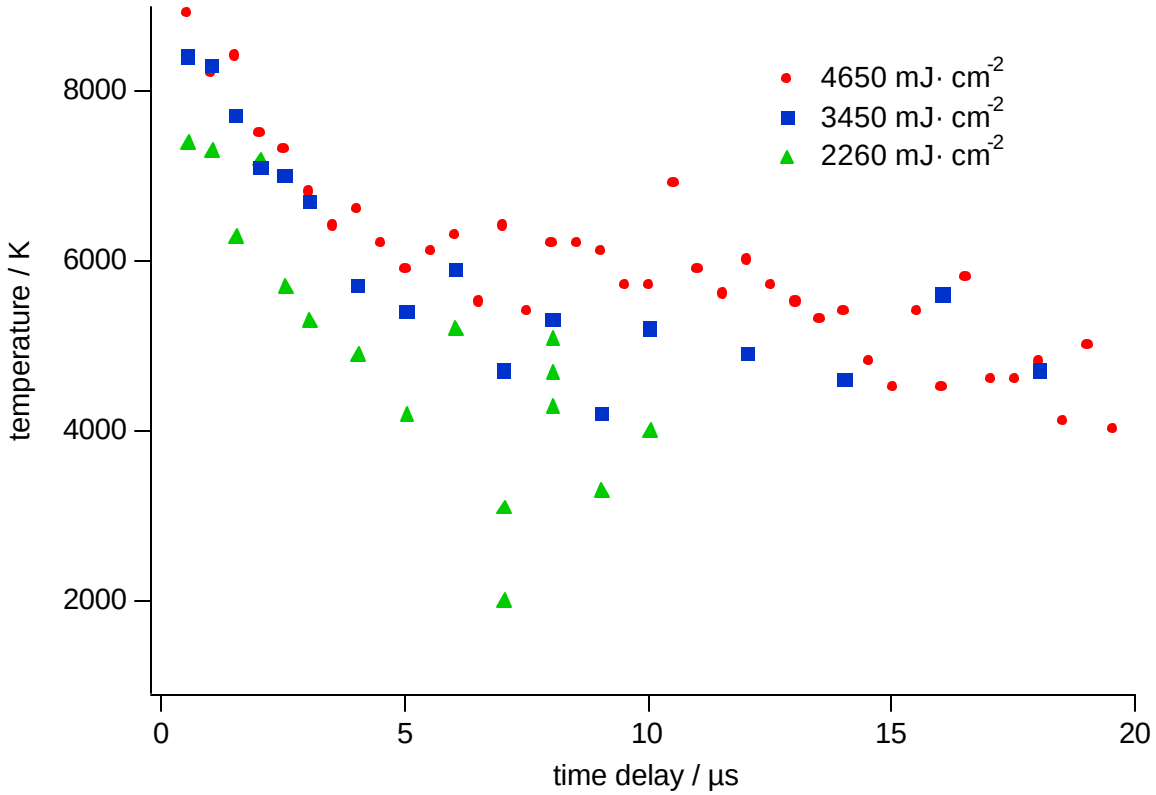

Figure 23: Decay of the plasma temperature with time for the thermalized simulation of the CN-violet system of GAP+C after irradiation with 193 nm and various fluences.

The ablation of GAP and PVC was probed after irradiation with 193 and 1064 nm at lower and higher fluences. At the lower fluences shadowgraphy is used as analytical tool, while in the high fluence range time-resolved emission spectroscopy has been applied. The shadowgraphy reveals pronounced differences in the shape and composition of the ablated products. PVC reveals mainly solid products, while GAP (and TP) show two different products, i.e. gaseous and larger fragments. In the case of PVC a very directional shape of the products is observed, where the product even overtake the shockwave. An analysis of the ablation crater revealed also, that PVC has in spite of the similar

absorption coefficient a much lower threshold fluence for ablation than GAP. The reasons for this behavior are not clear at the moment.

The emission spectra at the high fluence range were analyzed in detail, using a simulation routine to calculate the plasma temperature from diatomic species. The plasma temperatures were determined for 193 nm irradiation and GAP+C. The simulation yields initial plasma temperatures in the range of 8000 K, which decay within 5 µs to temperatures in the range of 4000- 5000 K.

Results IV: Emission-Spectroscopy

Various improvements of our emission spectroscopy setup made it possible to determine and compare the plasma characteristics (spectra and calculated temperatures) for PVC and GAP doped with carbon after irradiation at 1064 nm (6 ns pulses).

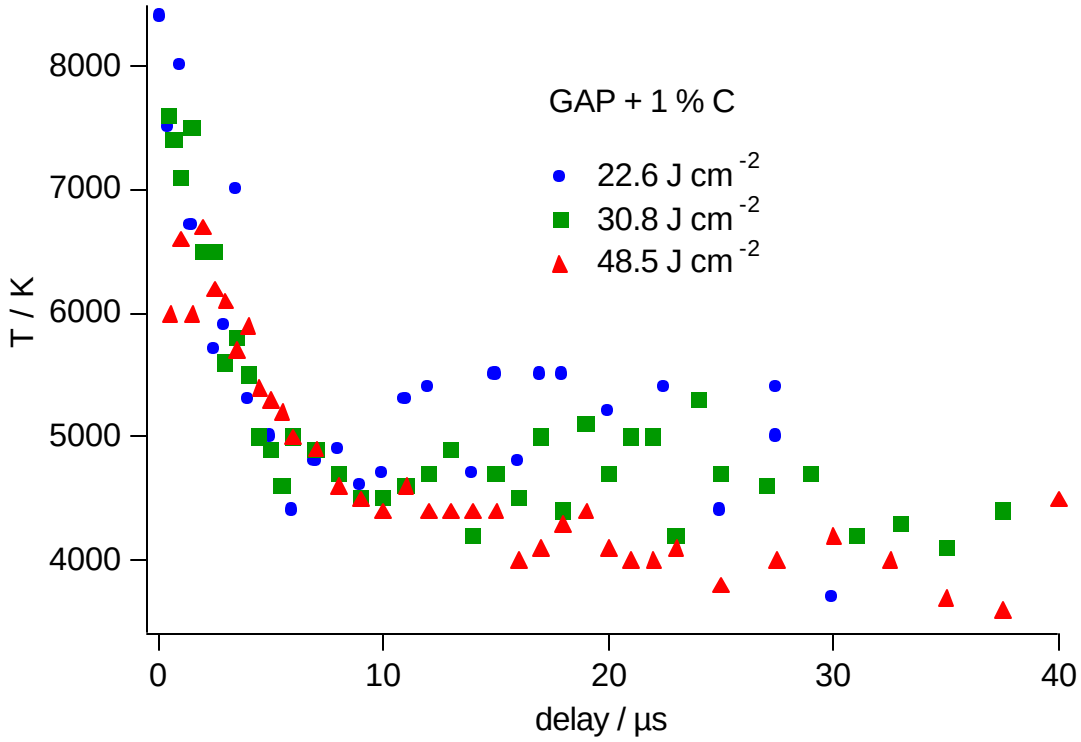

Figure 24: Decay of the plasma temperature with time for the thermalized simulation of the CN-violet system of GAP+C after irradiation with 1064 nm and various fluences.

The calculated plasma temperatures of GAP are shown in Figure 24 as function of time for different fluences. Two features are clearly visible in the graph:

- A fast decrease of the temperature for all fluences.
- A decrease of the initial plasma temperatures for increasing fluences.

The initial temperature of around 8000 K is comparable to the temperatures reached by 193 nm irradiation (also at much lower fluences, i.e. 4 vs. 20 J cm^{-2}, in the case of 193 nm irradiation). The decrease of the initial plasma temperature (of the CN species) with increasing laser fluences was not observed for 193 nm irradiation. This may be due to the much higher fluences applied at 1064 nm which are at least partially used for the creation of Bremsstrahlung (or breakdown of air). The background emission (Bremsstrahlung) increased with the increasing fluences (above 20 J cm^{-2}) at a much faster rate than the emission peaks.

The same behavior (lower intensity for higher fluences) is also observed for PVC, shown in Figure 25, but some differences are also clearly visible, i.e. the initial

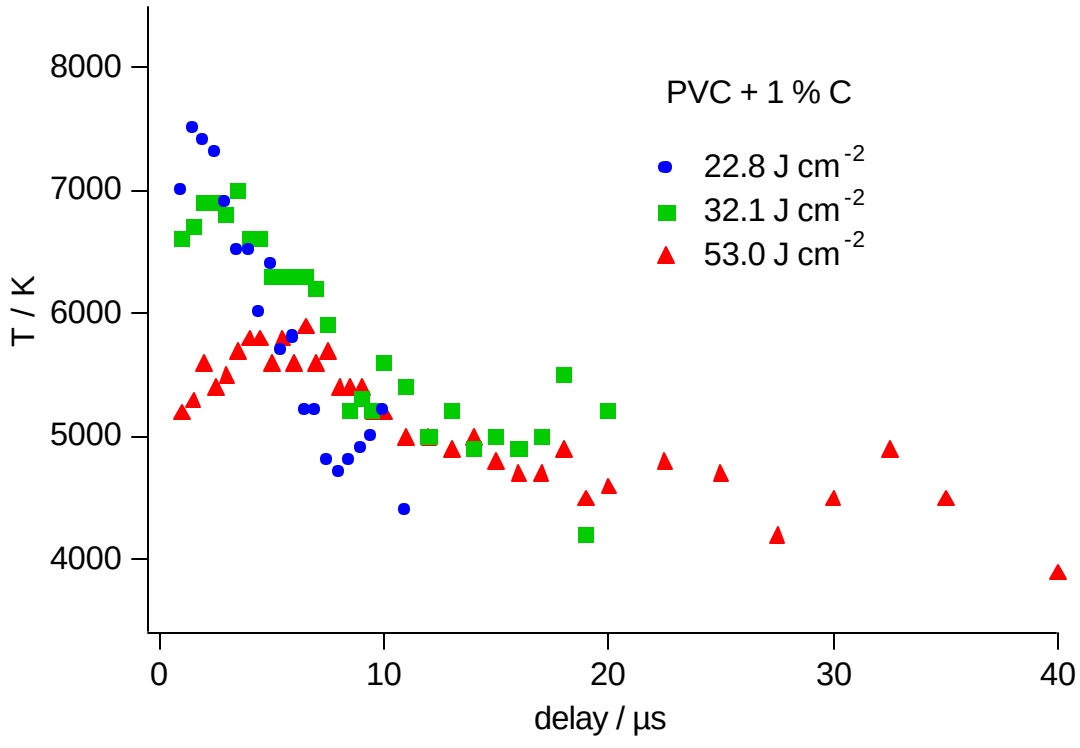

Figure 25: Decay of the plasma temperature with time for the thermalized simulation of the CN-violet system of PVC+C after irradiation with 1064 nm and various fluences.

temperatures are lower compared to GAP and the maximum temperatures are

reached later in time. The initial increase of the temperature to reach the maximum after 2-5 µs, is detected for all fluences, while in the case of GAP only a decaying temperature was obtained. This suggests that the maximum temperatures in the plasma are reached faster, implying also even higher temperatures than the value obtained in our calculations.

Another interesting feature of the plasma temperatures of GAP and PVC after 1064 nm irradiation (much less pronounced for 193 nm irradiation) was detected during the temperature analysis of the CN bands. A better correlation between the fits and the measured spectra were obtained when different rotational (T_{rot}) and vibrational temperatures (T_{vib}) were used (shown in Figure 26), which is clearly visible in the short wavelength tail that is mainly defined by T_{rot}.

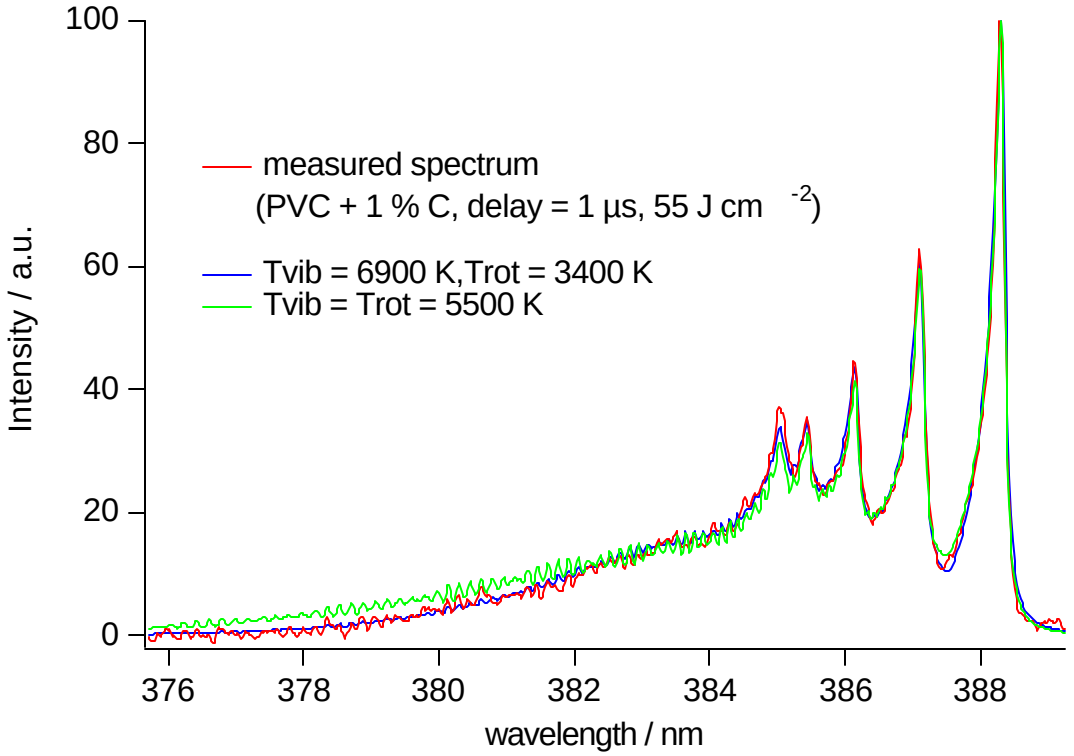

Figure 26: Emission spectra of PVC+C in the region of the CN violet system with added simulation of the spectrum assuming a thermalized and a system with different rotational and vibration temperatures.

The evolution of the temperatures (T_{rot} and T_{vib}) is shown in Figure 27 as function of the fluence for a fixed delay time. The rotational temperature is always lower than the vibrational temperature. The temperatures shown in all other graphs

were obtained for the fits with identical rotational and vibrational temperatures to allow an easier comparison by using only one temperature.

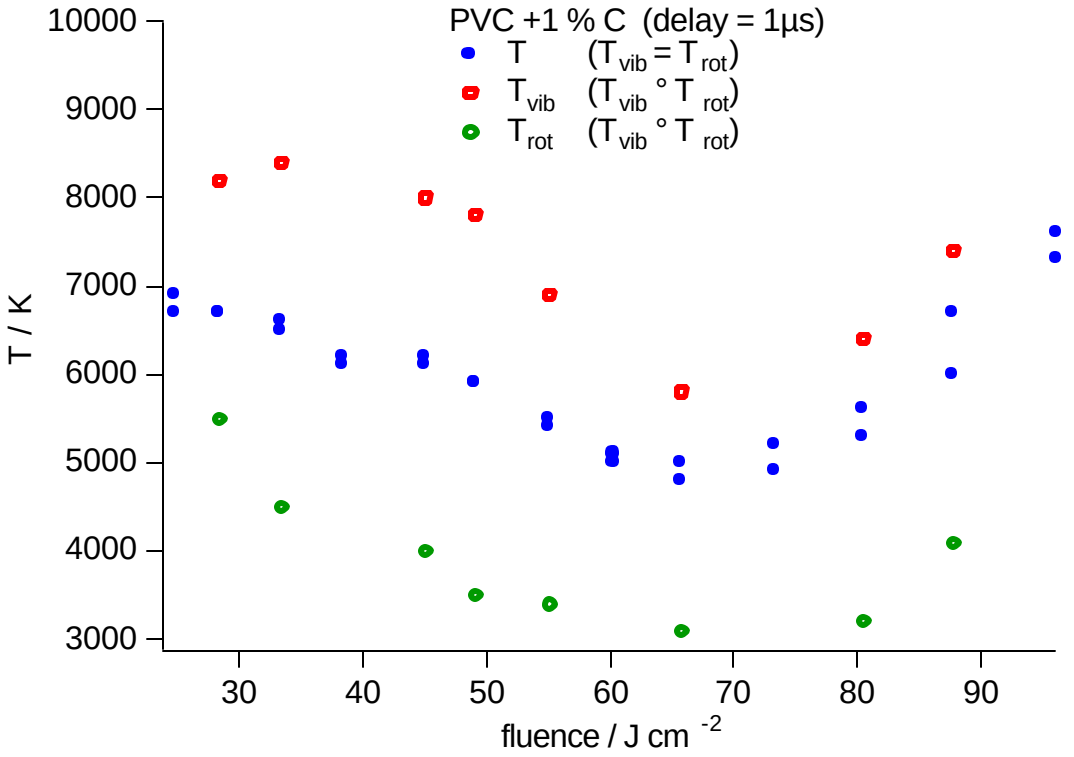

Figure 27: Decay of the rotational and vibrational temperatures after 1 µs for the simulation of the CN-violet system of PVC + C after irradiation with 1064 nm and various fluences.

The pronounced differences between GAP and PVC, i.e. the higher temperatures in the case of GAP (and the above described faster shockwaves) could be caused by or even be partially responsible for the higher thrust in LPT experiments of Claude Phipps. The different amount of ablated material between GAP and PVC in our experiments (with irradiation on the surface of the polymers vs. irradiation through the substrate in Claude Phipps experiments with approximately constant amount of material removal) are probably responsible for the different shock wave velocities (more gaseous material in the case of GAP), but not for the higher thrust in the experiments of Claude Phipps, where the complete polymer layer is removed (“burn-through”).

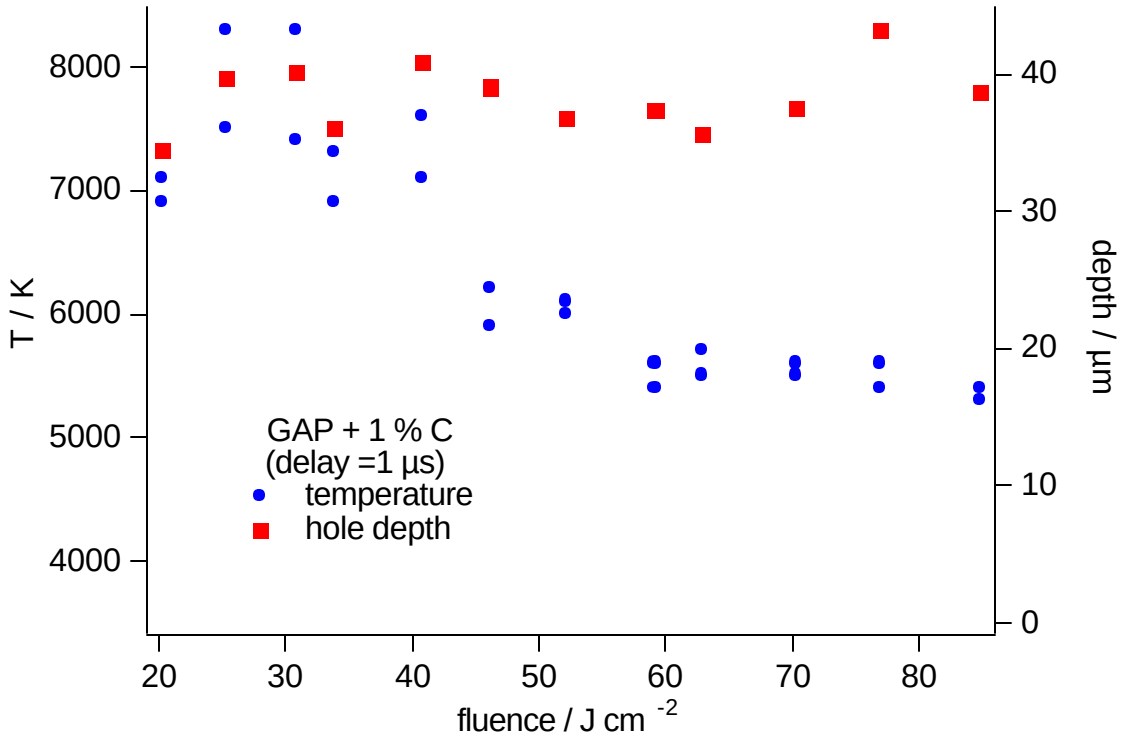

Figure 28: Decay of the plasma temperature and ablation depth after 1 µs for the thermalized simulation of the CN-violet system of GAP + C after irradiation with 1064 nm and various fluences.

Whether and how the amount of ablated material influences the plasma temperature could not be evaluated, because the amount of ablated material is constant at high fluences. This is most probably due to plasma-shielding that limits the number of photons reaching the surface. The laser photons are absorbed in the plasma and result in the above discussed higher intensity of the Bremsstrahlung that is not really probed and calculated in our measurements (we use the CN system for the calculations). The dependence of the plasma temperature on the fluences and the corresponding ablation depths are shown in Figure 28 (for GAP) and 29 for (PVC).

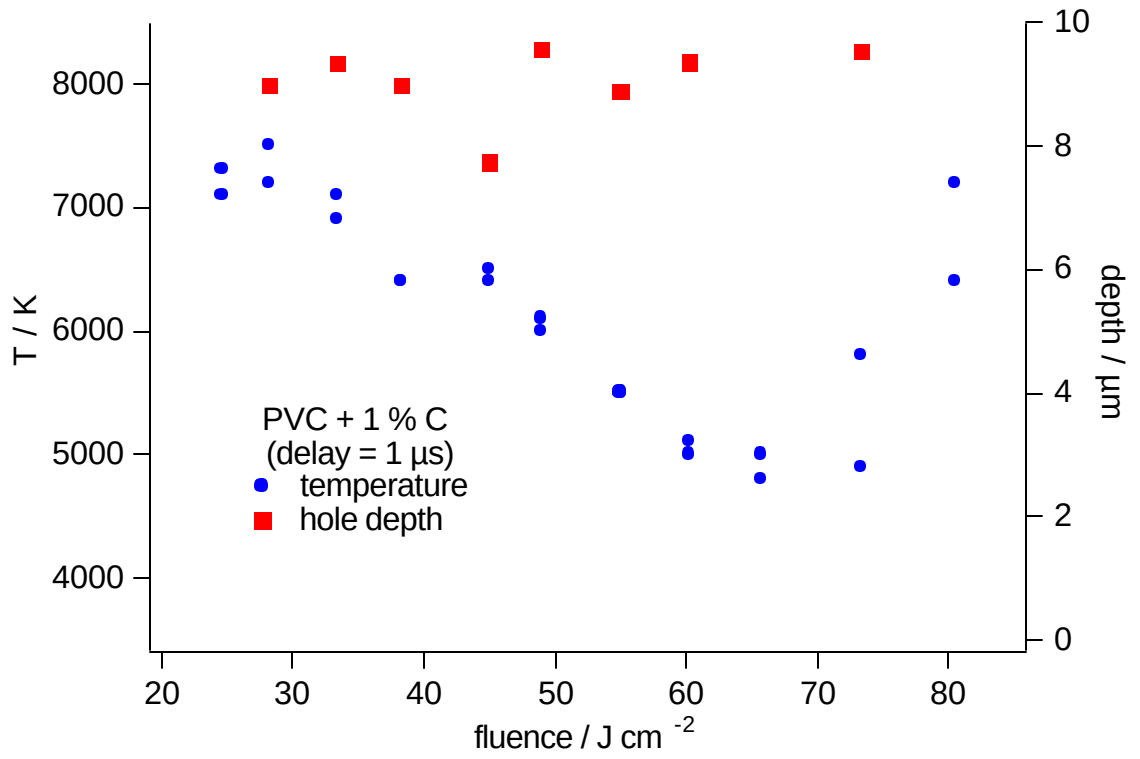

Figure 29: Decay of the plasma temperature and ablation depth after 1 µs for the thermalized simulation of the CN-violet system of PVC + C after irradiation with 1064 nm and various fluences.

The plasma temperatures of GAP and PVC decrease, as discussed above, with increasing fluences. PVC reveals additionally another unexpected behavior, i.e. an increase of the temperatures for fluences above 70 J cm^{-2}, which cannot be explained by effects such as breakdown in air (not observed for the same fluences with GAP). The ablation depths for PVC are much lower (roughly a factor of 4) compared to GAP as already shown in Figure 19. Emission spectra of the complete spectral range were measured (shown in Figure 30 and 31) to test whether the decay of the plasma temperature with increasing fluence is associated with spectral changes in the spectra. The most important feature is an increase of a broad band centered around 480 nm (marked yellow), which could not yet be clearly assigned. The intensity of this band increases with increasing fluences faster than all other band systems in the spectra.

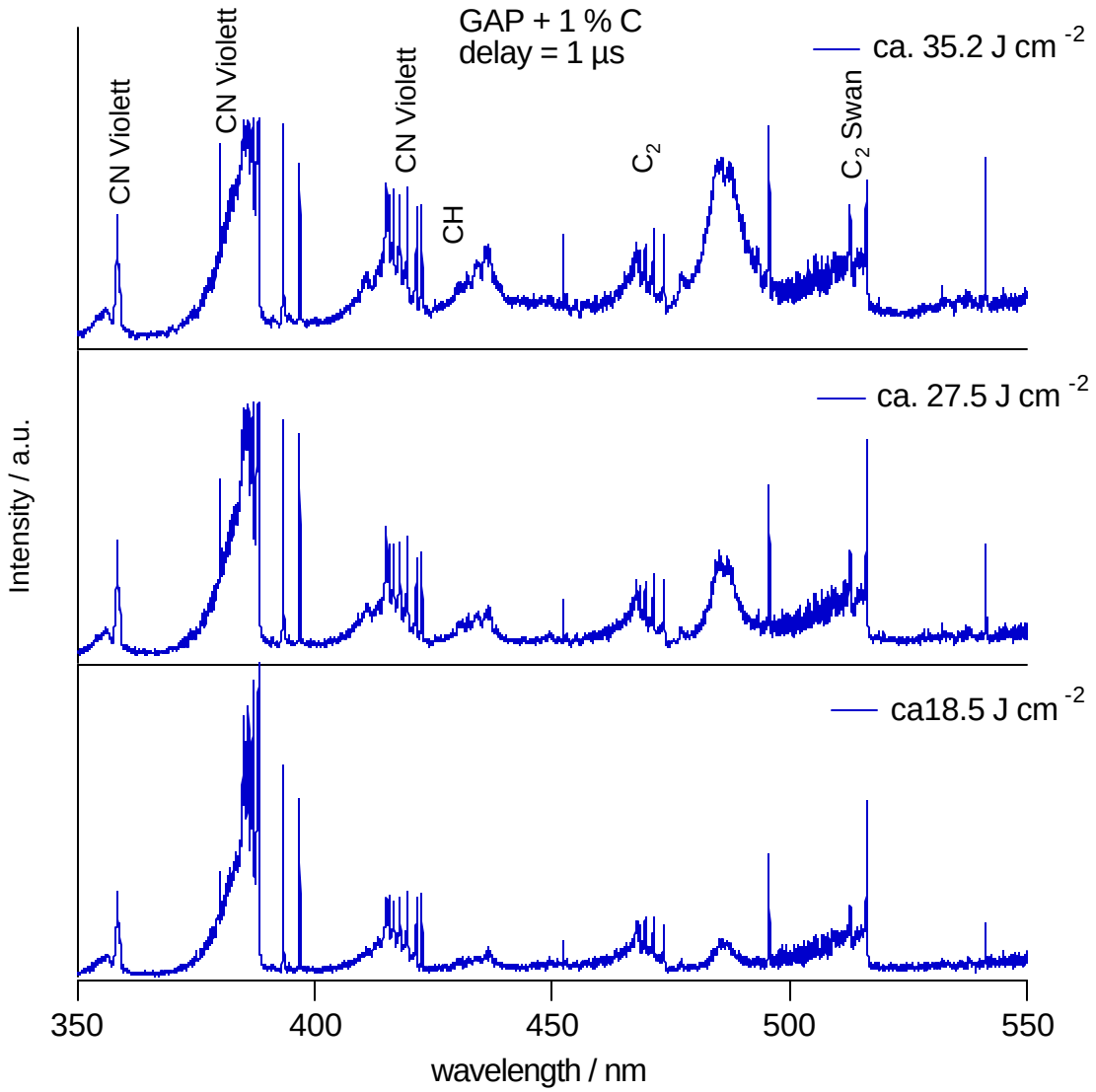

Figure 30: Emission spectra of GAP + C after irradiation with 1064 nm and various fluences.

A similar behavior, also with a less pronounced increase and an initial higher intensity, is observed for PVC + C (shown in Figure 31).

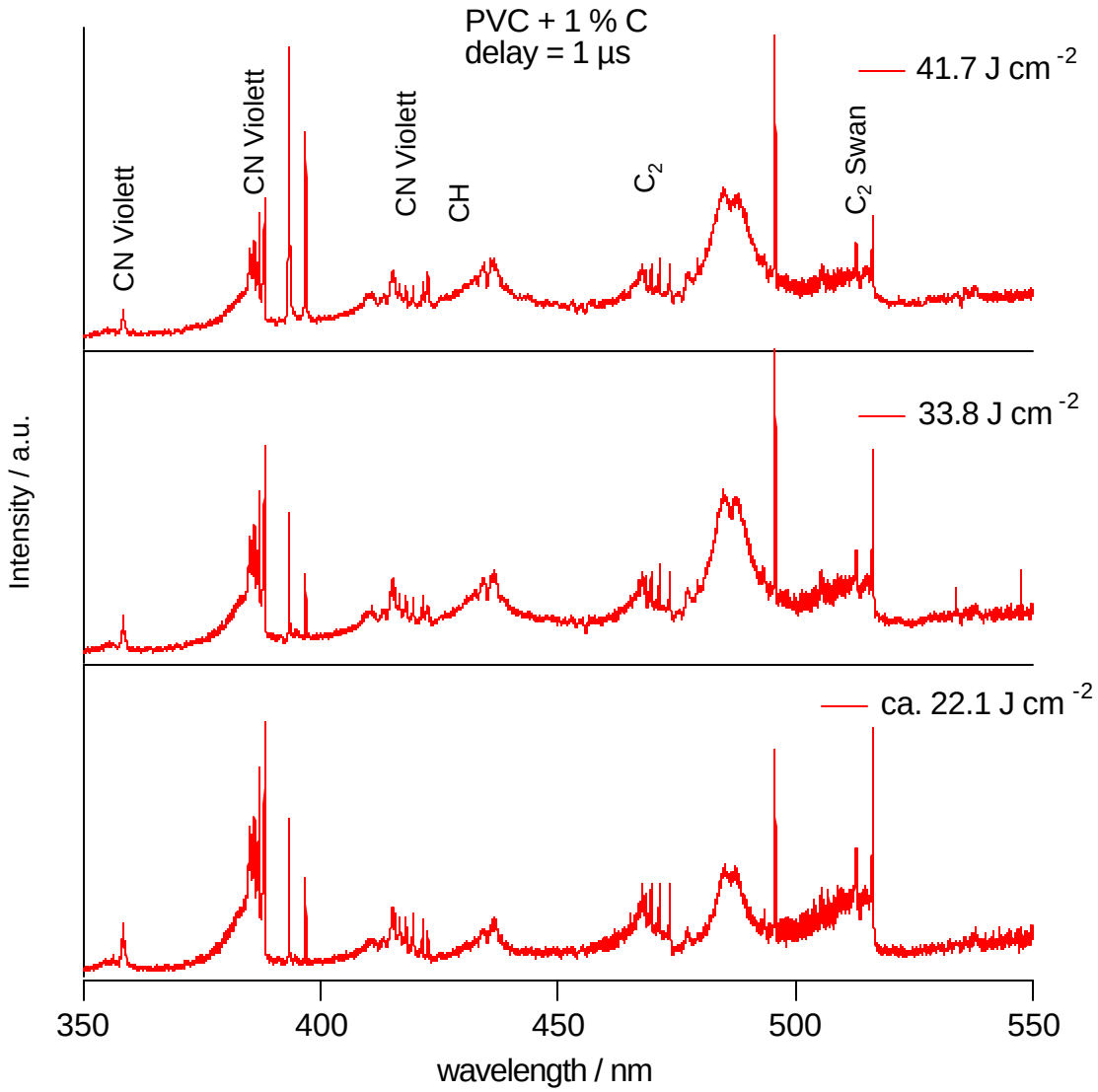

Figure 31: Emission spectra of PVC + C after irradiation with 1064 nm and various fluences.

The band system at 480 nm reveals an interesting temporal behavior, i.e. the intensity of the band decays faster than all other observed band systems (shown for GAP + C in Figure 32). The band disappears prior to 4 µs where all other bands are still clearly detectable.

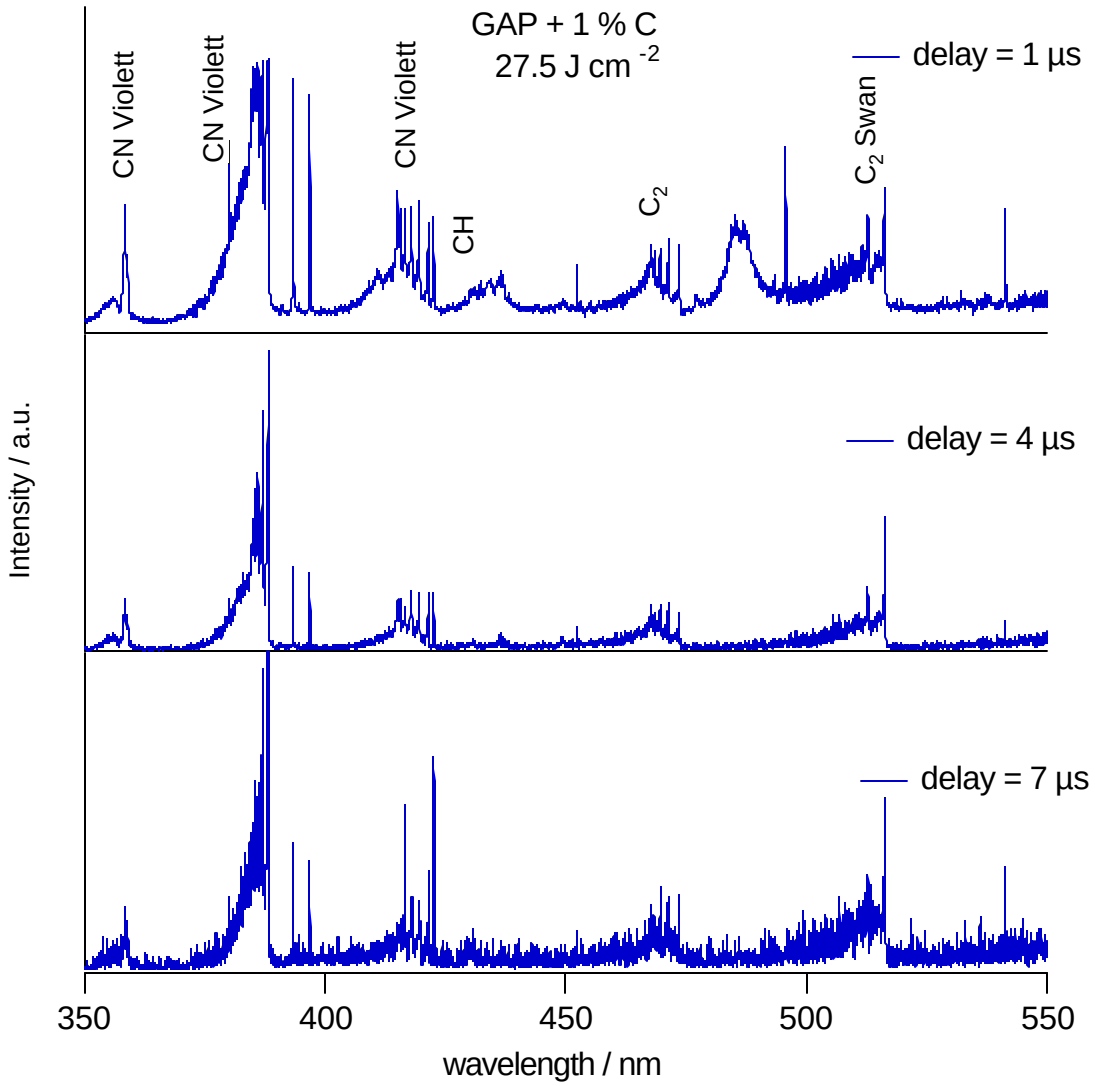

Figure 32: Emission spectra of GAP + C after irradiation with 1064 nm and various fluences.

Another important parameter, which we studied already initially, is the role of the dopant that creates the absorption in the near IR. We have focused our research on carbon as dopant for GAP, as we did initially not succeed in the preparation of GAP films with organic IR dyes. Organic dyes should be more or less molecular heaters, which are homogenously distributed through the polymer matrix (size = 1 nm), while the carbon particles may be considered as larger “hot spots” (due to agglomeration probably much larger then nominal particle size of 5-10 nm). The IR dyes are also selected for one important property, i.e. they show a fast (ps)

vibrational relaxation (efficient heating of the surrounding matrix). These special properties are used in their commercial application, e.g. as absorber in laser safety goggles. We have obtained new stable IR-dyes, and we succeeded in the preparation of GAP films with an IR-dye (*Epolight 2057)*, but the preparation procedure is still not really optimized. The absorption spectrum of a thin GAP film doped with the IR dye is shown in Figure 33, where the corresponding spectrum of a carbon-doped film is also included.

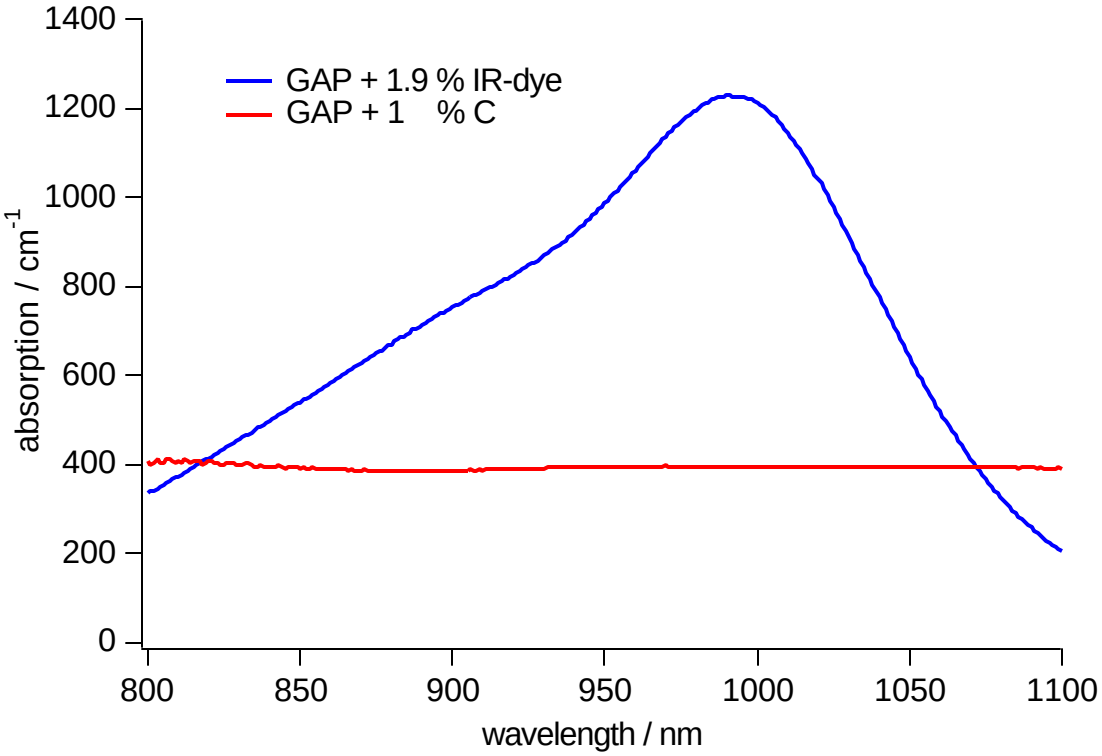

Figure 33: Absorption spectra of GAP doped with carbon and an IR-dye.

The GAP films doped with the IR dye were analyzed by emission spectroscopy, which already revealed pronounced differences between the films doped with carbon and the IR dye. The intensity of the diatomic emission bands for the films doped with the IR dye is lower (exemplified by the lower signal to noise ration of the spectra shown in Figure 34), while the plasma temperatures show two interesting features:

- The initial plasma temperatures are higher for the IR doped films (shown in Figure 35) compared to the C doped films (> 8000 K).
- Good fits are obtained for fitting the temperatures with identical rotational and vibrational temperatures (shown in Figure 36).

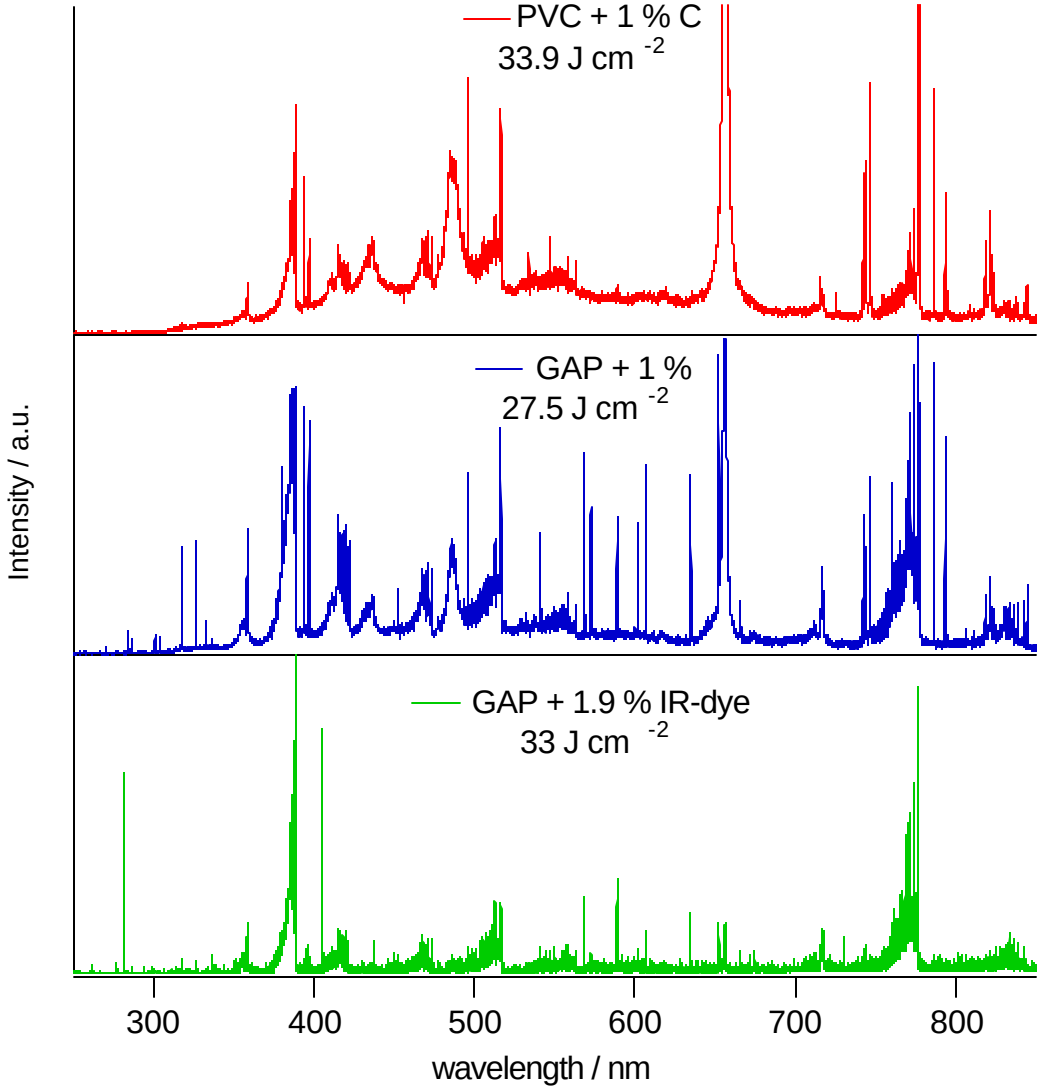

Figure 34: Emission spectra of PVC + C, and GAP doped with carbon and an IR-dye after irradiation at 1064 nm.

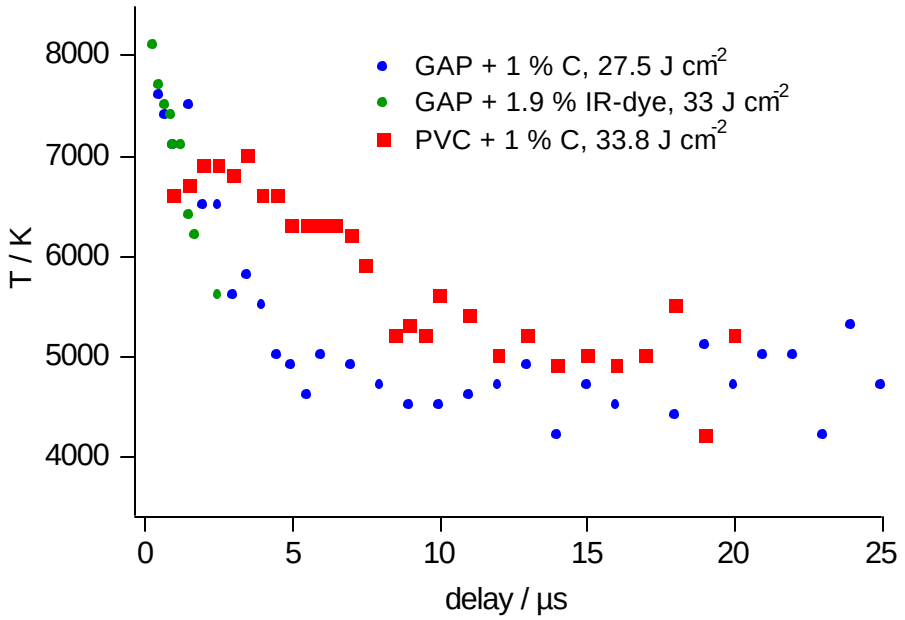

Figure 35: Decay of the plasma temperature with time for the thermalized simulation of the CN-violet system of PVC+C and GAP doped with carbon and an IR-dye after irradiation at 1064 nm.

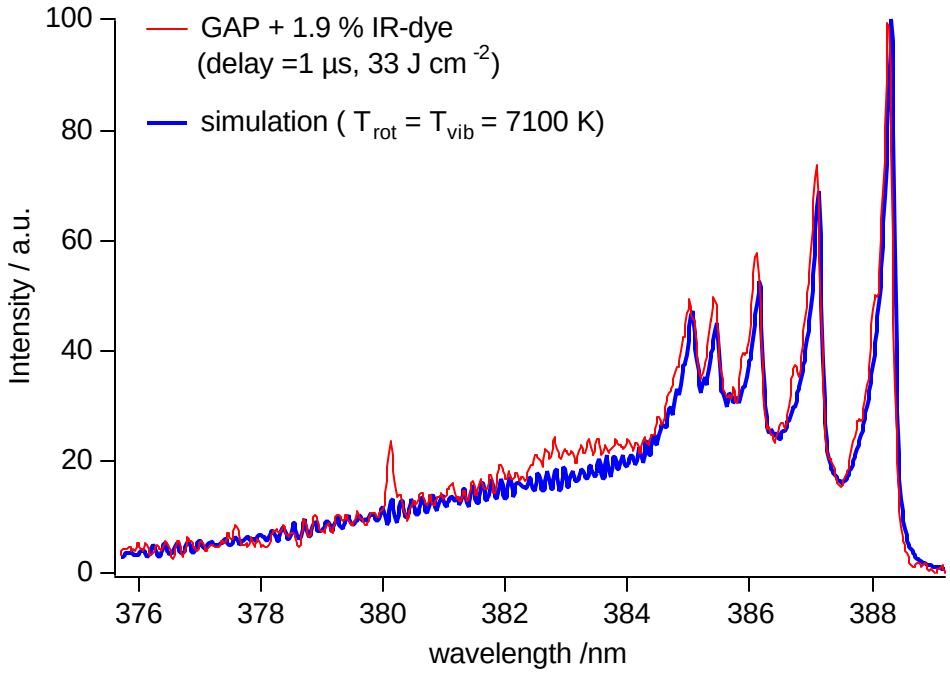

Figure 26: Emission spectra of PVC+C in the region of the CN violet system with added simulation of the spectrum assuming a thermalized and a system with different rotational and vibration temperatures.

Conclusions

Various polymers were tested for a possible application as fuels in laser plasma thrusters, where near IR irradiation wavelengths are utilized. Absorption in the near IR was utilized by doping of the films with carbon or an IR dye. The best carbon dopant, defined by thrust measurements, are carbon particles with a nominal size of 5-10 nm. The procedure for doping the polymers films by IR dyes was only developed shortly before the end of this contract, therefore only a limited amount of data is available. The films doped with the IR dye should have better properties, as a more homogeneous and efficient coupling of the laser energy in the matrix should be accomplished. Plasma temperature measurements support this assumption, as higher temperatures compared to carbon-doped films could be obtained. The tested polymers included standard commercial polymers, such as poly butadiene, poly vinylalcohol co-polymers and PVC (the best material identified by Claude Phipps), to polymers designed for laser ablation in the UV, and energetic polymers. The energetic polymers revealed much better properties than the PVC. Therefore a method was developed prepare films, including large films that can be applied in thrust measurements with tape geometry (performed by Claude Phipps).

The energetic materials and PVC were studied in detail with various methods to understand why the energetic material performed so much better in the thrust experiments by Claude Phipps. Ablation experiments at 1064 nm (with ns pulses) revealed unexpectedly that PVC has a lower threshold of ablation, but also lower ablation rates than the energetic polymer (GAP). Time-resolved studies using ns shadowgraphy, where the speed of the shock wave is analyzed, suggested that higher shock wave velocities with less solid fragments are obtained for GAP compared to PVC. This is probably due to the larger amount of gaseous product which result in a higher pressure of the products that support the shock wave. These measurements were performed at laser fluences which are below the threshold of plasma creation, which is of course an important for the thrust experiments. Therefore experiments at higher fluences were performed were a plasma was observed. The plasma was analyzed by time-resolved emission

spectroscopy, and the CN system was used to calculate plasma temperatures. Again pronounced differences were found between PVC and GAP, i.e. higher temperatures were reached on a faster time scale for GAP. This could be directly be related to the better performance of GAP in the thrust experiments. Another interesting feature that was observed is the decrease of the plasma temperature with increasing laser fluence, which is probably due to the more pronounced creation of Bremsstrahlung. It is also very interesting that the ns experiments image the behavior of the thrust measurements where ms pulses are applied.

Outlook:

- Possible future measurements should include thrust measurements with ns pulses (by C. Phipps), and plasma measurements with ms pulses.
- Optimization of the preparation of the IR dye doped films and their characterization.
- Determination of the thermal properties of GAP + C and PVC + C films.

Acknowledgements

The cooperation of Claude Phipps, who was always a most helpful partner in discussions and who performed all thrust measurements is gratefully acknowledged.